mock vector was used as a control. A 4-[3-(4-iodophenyl)-2-(4-nitrophenyl)-2H-5-tetrazolio]-1,3-benzene disulfonate (WST-1)-based cell proliferation assay (Roche Diagnostics) was performed 48 h after differentiation. Absorbance was measured in a multiple plate reader (PowerscanHT, Dainippon Pharmaceutical, Japan). The assay was carried out in triplicate and statistically analyzed by one-way analysis of variance or unpaired *t* test.

*Quantitative Analysis of Gene Expression Levels*—Total RNA was extracted from Neuro-2a cells expressing SOD1-GFP and their Cys to Ser derivatives by using an RNA Easy Kit (Qiagen), followed by cDNA synthesis primed with oligo(dT) using Superscript II (Invitrogen). The gene expression level was examined by quantitative reverse transcription-PCR using primer sets specific to target genes and QuantiTect SYBR Green PCR kit (Qiagen). PCR was performed on an iCycler system (Bio-Rad) under the manufacturer's recommended conditions.

*Isolation of SOD1 Aggregates*—Isolation of SOD1 inclusion bodies was carried out according to Lee *et al.* (24) with a slight modification. $5 \times 10^5$ Neuro-2a cells in a 60-mm dish expressing SOD1-GFP were washed with cold phosphate-buffered saline before addition of TNE buffer. After a 5-min incubation at room temperature, the supernatant containing Nonidet P-40-soluble proteins was carefully removed from dishes. After gentle washing of dishes with phosphate-buffered saline, the Nonidet P-40-insoluble materials were scraped and incubated on ice for 5 min. The extract was then centrifuged at $80 \times g$ for 15 min. The pellet containing big inclusions was put onto a slide glass, sealed with a coverslip, and observed under a BX51 epifluorescence microscope (Olympus, Tokyo, Japan).

*Cycloheximide Chase Analysis*—Neuro-2a cells grown on 6-cm dishes were transfected with 1 μg of pcDNA3.1/MycHis-SOD1 with or without 1 μg of pcDNA4/HisMax-Dorfin. 24 h after transfection, cycloheximide (50 μg/ml) was added to the culture medium, and the cells were harvested at the indicated time points. The samples were subjected to SDS-PAGE and analyzed by Western blotting with anti-Myc antibody. The intensities of the bands were quantified by ImageGauge software (Fuji Film, Tokyo, Japan). The assay was carried out in triplicate and statistically analyzed by one-way analysis of variance or unpaired *t* test.

## RESULTS

*Proteasome Inhibition Increases SDS-resistant Disulfide-linked Species as Well as Insoluble Ones of ALS-linked Mutant SOD1*—Mutant SOD1 is a fairly unstable protein, and the increased turnover of mutant SOD1 is mediated by the ubiquitin-proteasome pathway (18, 19). Thus, we first examined the effect of proteasome inhibition on mutant SOD1 proteins. When cellular proteasome activity was blocked by the proteasome inhibitor MG132, the level of soluble mutant $SOD1^{G85R}$ and $SOD1^{G93A}$ increased in a dose-dependent manner (Fig. 1*B*, *arrowhead*), and an SDS-resistant mutant SOD1 dimer appeared (Fig. 1*B*, *arrow*). The increase in the amount of wild-type SOD1 was much smaller than that of mutant SOD1 (Fig. 1*B*, *arrowhead*). Detergent-insoluble, sedimentable mutant SOD1 also increased as proteasome activity was inhibited (Fig. 1*C*). Interestingly, as the proteasome activity was inhibited, aberrant high molecular weight SDS-resistant disulfide-linked mutant $SOD1^{G85R}$ and $SOD1^{G93A}$ became more abundant (Fig. 1*A*, *asterisk*). There were almost no SDS-resistant disulfide-linked species of the wild-type SOD1. The same findings were obtained when blots were probed with anti-SOD1 antibody (supplemental Fig. S1*A*). These results were also confirmed with epoxomicin, a selective and irreversible proteasome inhibitor (supplemental Fig. S1*B*). Thus, intermolecular disulfide bond-linked mutant SOD1 is unstable and prone to degradation by the proteasome.

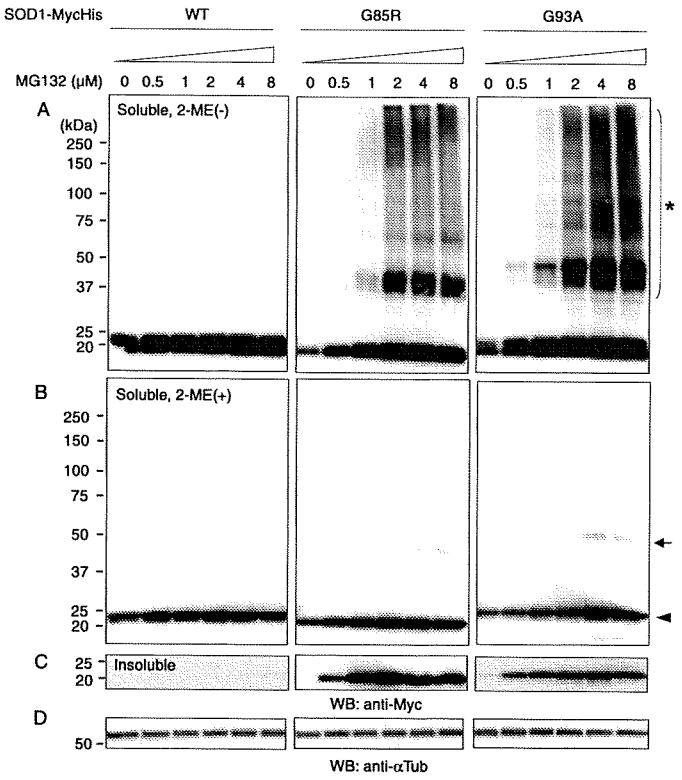


FIGURE 1. **Proteasome inhibition leads to the accumulation of intermolecular disulfide bond-linked mutant SOD1.** Neuro-2a cells expressing wild-type (*WT*), G85R, and G93A mutant SOD1-MycHis were treated with MG132 for 24 h at the indicated concentrations. Soluble fractions were analyzed by SDS-PAGE in the absence (*A*) or presence (*B*) of 2-ME. Insoluble fractions were analyzed by SDS-PAGE in the presence of 2-ME (*C*). *Arrow*, a soluble SDS-resistant dimer; *arrowhead*, a soluble monomeric SOD1; *asterisk*, disulfide-linked high molecular weight-species of SOD1. *D*, anti-α-tubulin as loading control.

*Free $Cys^6$ and $Cys^{111}$ Are Important for Generating Disulfide Bond-linked Species and Insoluble, Sedimentable Forms of Mutant Human SOD1*—We examined the role of Cys residues in the formation of aberrant disulfide-bond linked high molecular weight species. Various combinations of the four Cys residues at positions 6, 57, 111, and 146 replaced with serines were introduced into SOD1 protein-expression vectors using site-directed mutagenesis. The effects of amino acid replacement at one of the four Cys residues, at two of the four Cys residues, and at all four Cys residues on wild-type and two familial ALS-linked SOD1 mutants, $SOD1^{G85R}$ and $SOD1^{G93A}$, were investigated. We used Myc-His-tagged SOD1 expression vectors and an antibody against the tag peptide to detect SOD1 protein so as to avoid possible reduced detection of SOD1 with multiple

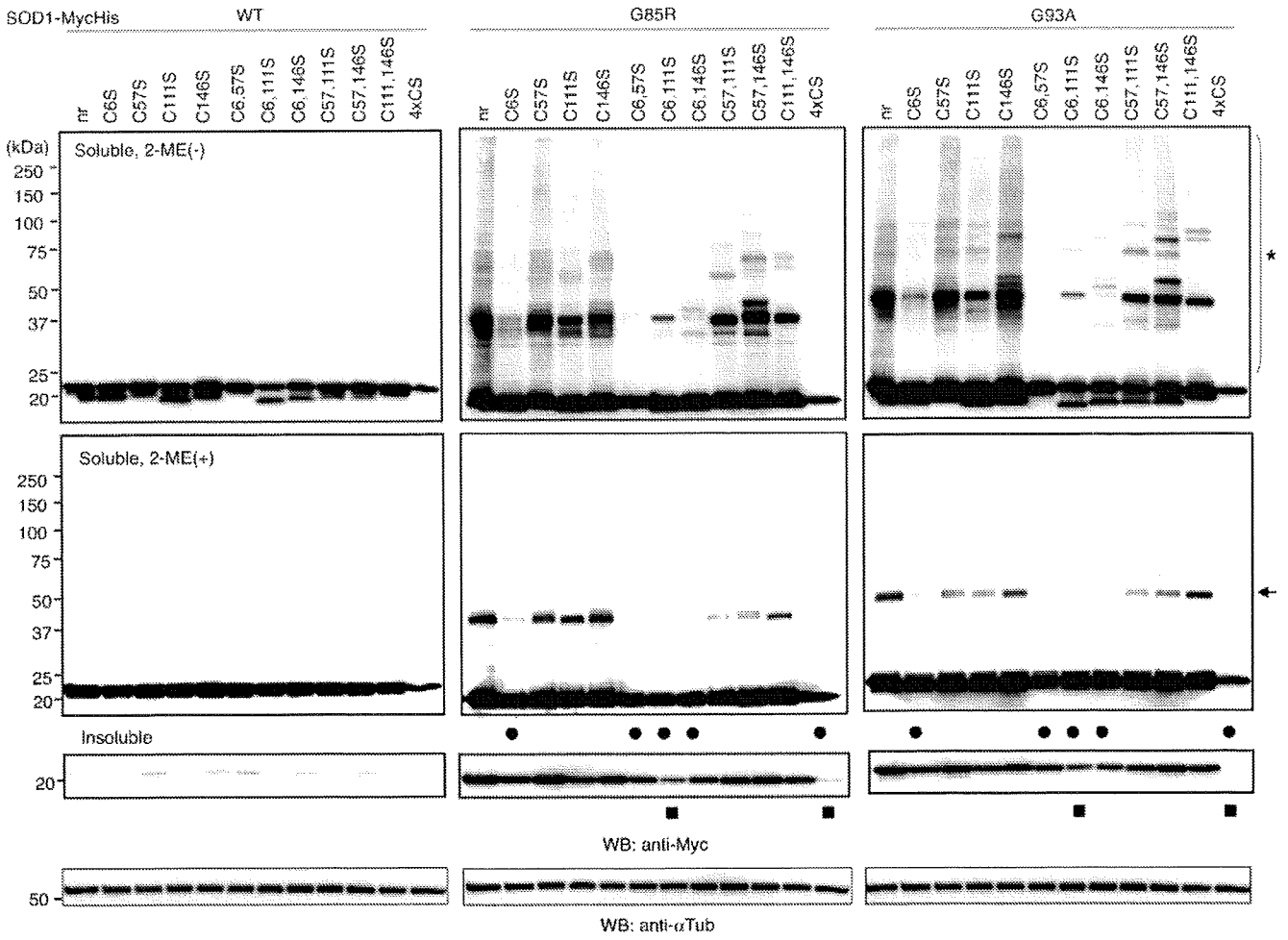


FIGURE 2. **Free Cys$^6$ and Cys$^{111}$ are important for generating intermolecular disulfide-linked species and insoluble, sedimentable forms of mutant human SOD1.** Various combinations of replacing Cys with Ser were introduced into wild-type (*WT*) and mutant (G85R and G93A) SOD1-MycHis. Neuro-2a cells expressing SOD1-MycHis were treated with 2 $\mu$M MG132 for 24 h. Soluble fractions were analyzed by SDS-PAGE in the absence (*upper panels*) or presence (*middle panels*) of 2-ME. Insoluble fractions were analyzed by SDS-PAGE in the presence of 2-ME (*lower panels*). *Asterisk*, a disulfide-linked high molecular weight species; *arrow*, an SDS-resistant dimer of mutant SOD1. *Filled circles*, marked reduction of an SDS-resistant dimer with a Cys$^6$ replacement of mutant SOD1; *filled squares*, further reduction of the detergent-insoluble, sedimentable form of mutant SOD1 with simultaneous Cys$^6$ and Cys$^{111}$ replacements. *nr*, SOD1 without replacement in cysteine residue; *4×CS*, all four cysteines replaced by serines.

amino acids changes by the anti-SOD1 antibody. Interestingly, none of the Cys residue replacements generated disulfide-linked species in wild-type SOD1 proteins (Fig. 2, *left panel*). Under reducing conditions, replacement of Cys$^6$ had a stronger effect on the formation of disulfide-linked species of mutant SOD1 than did the other three Cys residue replacements (Fig. 2, *middle* and *right panels, asterisk*). Combinations of replacing Cys$^6$ and one of the other Cys residues further attenuated the aberrant disulfide-linking of mutant SOD1 seen with the single substitution of Cys$^6$ (Fig. 2, *filled circle*). Under usual reducing conditions, the same reduced oligomerization of mutant SOD1 was observed when combinations of Cys$^6$ and other Cys residues were replaced (Fig. 2, *arrow*). The detergent-insoluble, sedimentable form of mutant SOD1 was also reduced especially if both Cys$^6$ and Cys$^{111}$ were replaced (Fig. 2, *filled square*). Replacement of all four Cys residues completely abolished the disulfide-linked species in the non-reducing condition and the oligomeric, detergent-insoluble form of mutant SOD1 in the reducing condition (Fig. 2, *lane 4×CS*). Because simultaneous substitutions of Cys$^6$ and Cys$^{111}$ had the strongest effects on the formation of aberrant species of mutant SOD1 in both non-reducing and reducing conditions, we compared C6S and C111S mutants with C57S and C146S mutants in the following experiments.

*Substituting Both Cys$^6$ and Cys$^{111}$ Greatly Reduces High Molecular Weight Aggregate Formation and Ubiquitylation of Mutant SOD1*—In studies of polyglutamine disorders, it has been demonstrated that high molecular weight aggregates of mutant proteins are retained by filtration through cellulose acetate (25, 26). Cellulose acetate membranes usually bind protein very poorly and are used to trap high molecular weight structures from complex mixtures through filtration. This assay was also successfully applied to detect mutant SOD1 aggregation (27). Thus we used a cellulose acetate filter trap assay to investigate whether SOD1 proteins with Cys substitutions are retained in high molecular weight aggregates from lysates of SOD1-MycHis expressing Neuro-2a cells. Cells were lysed in TNE buffer, fractionated into crude denucleated, soluble, and insoluble fractions, and each fraction was then filtered through a 0.22-$\mu$m cellulose acetate membrane. Subsequent staining

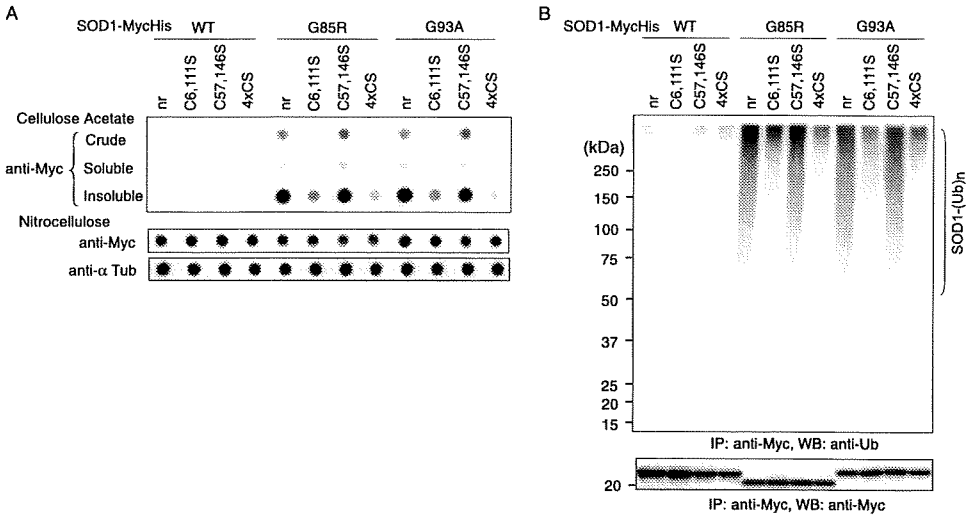


FIGURE 3. **Replacing both Cys$^6$ and Cys$^{111}$ greatly reduces high molecular weight aggregate formation and ubiquitylation of mutant SOD1-MycHis.** *A*, crude, soluble, and insoluble fractions of cell lysates were analyzed by filter trap assay (*upper panel*). Nitrocellulose dot blots probed with anti-Myc (*middle panel*) and anti-α-tubulin (*lower panel*) antibodies were used as loading controls. *B*, *in vivo* ubiquitylation assay. Western blotting of SOD1-Myc-His immunoprecipitates with anti-ubiquitin antibody demonstrated polyubiquitylation of mutant SOD1s and their C57, 146S derivatives. Replacement of Cys$^6$ and Cys$^{111}$ abolished polyubiquitylation of mutant SOD1. *nr*, SOD1 without replacement in cysteine residue; *4×CS*, all four cysteines replaced by serines.

with anti-Myc antibody revealed trapped SOD1 proteins (Fig. 3*A*, *upper panel*). Interestingly, high molecular weight aggregates were abundantly detected in mutant SOD1$^{G85R}$, SOD1$^{G93A}$, and their C57S and C146S derivatives. Replacements of Cys$^6$ and Cys$^{111}$ greatly reduced high molecular weight structures of mutant SOD1. No high molecular weight aggregates were present in either wild-type SOD1 or their Cys-substituted mutants.

Mutant, but not wild-type, SOD1 is conjugated to a multiubiquitin chain and degraded at the proteasome (20, 28). To assess whether SOD1 proteins are ubiquitylated, we carried out an *in vivo* ubiquitylation analysis by expressing SOD1$^{WT}$, SOD1$^{G85R}$, SOD1$^{G93A}$, and their Cys to Ser mutants in Neuro-2a cells in the presence of the proteasome inhibitor MG132. When SOD1 was then immunoprecipitated, mutant SOD1s, but not wild-type SOD1, were polyubiquitylated (Fig. 3*B*, *lane 1*). Replacement of both Cys$^6$ and Cys$^{111}$ abolished ubiquitylation of mutant SOD1, whereas replacement of Cys$^{57}$ and Cys$^{146}$ did not affect the ubiquitylation status of mutant SOD1 (Fig. 3*B*, *lane 2 versus lane 3*). Wild-type SOD1 and its Cys-replacement mutants were not ubiquitylated at all. Replacing only one of the four Cys residues attenuated neither the formation of high molecular weight species nor the ubiquitylation of mutant SOD1 (data not shown). Thus, the presence of both Cys$^6$ and Cys$^{111}$ is important for high molecular weight aggregate formation and ubiquitylation of mutant SOD1. Disulfide bond formation at Cys$^6$ or Cys$^{111}$ is critical step for ubiquitylation of mutant SOD1.

*Formation of Disulfide-linked Species of Mutant SOD1 Strongly Correlates with Visible Aggregate Formation and Neurotoxicity*—Expression of mutant, but not wild-type, SOD1 induces large perinuclear intracytoplasmic aggregates in differentiated Neuro-2a cells and reduces cellular viability (20). We analyzed the role of mutant SOD1 Cys residues in aggregate formation and neurotoxicity in Neuro-2a cells. Replacements of Cys$^6$ and Cys$^{111}$ significantly reduced the percentage of mutant SOD1$^{G85R}$ and SOD1$^{G93A}$ cells with visible aggregates (Fig. 4*A*). To further demonstrate the extent of aggregate formation, we isolated SOD1 aggregates with a procedure according to Lee *et al.* (24). Differentiated Neuro-2a cells bearing SOD1-GFP aggregates were extracted with 1% Nonidet P-40 in the culture dish, and the Nonidet P-40-soluble proteins were gently removed. Under this condition, the soluble monomeric SOD1 was completely removed, and the aggregates remained in the culture dish due to their association with unknown structures (24). The remaining Nonidet P-40-insoluble portion was then scraped and centrifuged at 80 × *g*. After the centrifugation at 80 × *g* for 15 min, the pellet fraction was found to contain exclusively the large inclusion bodies. Replacements of Cys$^6$ and Cys$^{111}$ markedly reduced the number of inclusion bodies in G93A mutant SOD1-GFP (Fig. 4*B*). Mutant SOD1$^{G85R}$ and SOD1$^{G93A}$, but not wild-type SOD1, are toxic in differentiated Neuro-2a cells as previously described (20). However, replacement of the Cys$^6$ and Cys$^{111}$ residues markedly reduced this neurotoxicity (Fig. 4*C*), which was not affected by replacing the Cys$^{57}$ and Cys$^{146}$ residues. There were no significant differences among the expression levels of all the constructs (Fig. 4*D*). Thus, changes in inclusion formation and toxicity are not due to differences in altered expression. These results provide evidence of direct links among intermolecular disulfide bonding, ubiquitylated complex formation, visible aggregate formation, and neurotoxicity.

*Preferential Occurrence of Disulfide-cross-linked Mutant SOD1 in the Affected Lesions of ALS Model Mice*—Although mutant SOD1 is expressed at similar levels in both neuronal and non-neuronal tissues, the aggregated and ubiquitylated forms are selectively found in the pathological lesions of patients and mutant SOD1-transgenic mice (29, 30). Thus, we next examined whether mutant SOD1 is aberrantly disulfide-linked in various tissues from symptomatic mutant SOD1 transgenic mice. Western blotting analysis, using anti-SOD1 antibody under reducing and non-reducing (omitting reducing agent 2-ME) conditions, demonstrated that the expression levels of mutant SOD1 were nearly the same in all tissues examined. Each of the tissues showed some of the disulfide-linked mutant SOD1species; however, in the brain stem and spinal cord, the areas predominantly affected in mutant SOD1-linked ALS, there was increased formation of intermolecular disulfide-linked species of mutant SOD1 (Fig. 5). Thus, intermolecular disulfide-linked

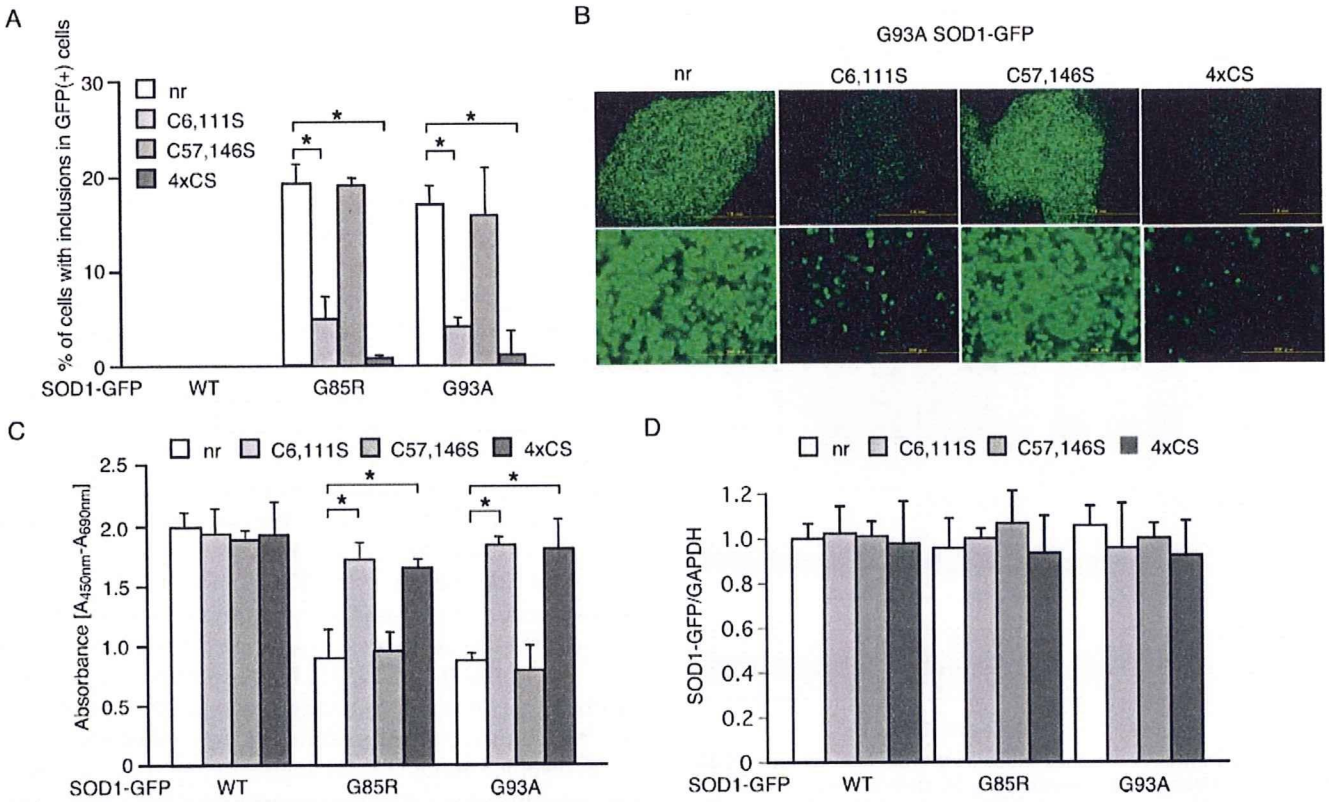


FIGURE 4. **Formation of disulfide-linked species of mutant SOD1 strongly correlates with visible aggregate formation and neurotoxicity.** *A*, the frequency of inclusion-bearing cells transfected with wild-type (*WT*), G85R, and G93A mutant SOD1-GFP and their Cys to Ser derivatives. *B*, G93A mutant SOD1-GFP inclusion bodies in 80 × *g* pellet. *Lower panels* are a high magnification image of the portion on the *upper panels* showing the whole pellet. The *scale bar* is equivalent to 10 mm in the *upper panels*, and 200 μm in the *lower panels*. *C*, change in the neurotoxic effect of mutant SOD1-GFP by Cys replacements to Ser. Cell viability was measured by the WST-1-based assay. *D*, all the constructs have equal expression. Transcription levels of SOD1-GFP in Neuro-2a cells expressing WT, G85R, and G93A mutant SOD1 and their Cys to Ser derivatives were examined by quantitative reverse transcription-PCR. Data were normalized with glyceraldehyde-3-phosphate dehydrogenase expression and then represent relative expression levels compared with levels in cells expressing WT SOD1-GFP. Data are mean ± S.D. values of triplicate assays. Statistical analyses were carried out by analysis of variance. *, $p < 0.01$. *nr*, SOD1 without replacing cysteine residues; *4×CS*, all four cysteines replaced by serines.

species are implicated as the aggregation-prone and neurotoxic intermediate of mutant SOD1 *in vivo*.

*Effects of Cys$^6$- and Cys$^{111}$-mediated Disulfide Linking on the Rate of Mutant SOD1 Degradation*—To determine whether replacement of Cys residues affects the degradation of SOD1 proteins, we examined the stability of mutant SOD1 proteins expressed in Neuro-2a cells (Fig. 6, *A* and *B*). Chase experiments with cycloheximide, which halts all cellular protein synthesis, demonstrated that replacement of Cys residues did not influence the stability of wild-type SOD1 protein (Fig. 6*A*). By contrast, although mutant SOD1 showed the enhanced degradation compared with wild-type proteins previously described (18–20), when both Cys$^6$ and Cys$^{111}$ were replaced with Ser, the degradation of mutant SOD1 was markedly increased (Fig. 6*B*). Replacement of Cys$^{57}$ and Cys$^{146}$ did not significantly change the rate of degradation compared with Cys-native mutant SOD1 protein.

*Ubiquityl Ligase Dorfin Ubiquitylates and Promotes Degradation of Disulfide-linked Mutant SOD1*—We have previously shown that Dorfin physically binds and ubiquitylates various familial ALS-linked SOD1 mutants and enhances their degradation (20). Thus, we examined whether Cys residues on SOD1 affect the binding and ubiquitylating activities of Dorfin. To this end, Dorfin was co-expressed with wild-type or mutant SOD1 in Neuro-2a cells. Dorfin co-immunoprecipitated with G85R and G93A mutant SOD1s and their Cys$^{57}$- and Cys$^{146}$-replaced derivatives (Fig. 7*A*). However, Dorfin interacted with Cys$^6$- and Cys$^{111}$-replaced mutant SOD1 only very weakly and failed to bind to mutant SOD1 when all four Cys residues were replaced (Fig. 7*A*). Dorfin did not bind at all to wild-type SOD1. Using an *in vivo* ubiquitylation assay, we further examined whether co-expressed Dorfin enhances the ubiquitylation of Cys-substituted mutant SOD1 (Fig. 7*B*). When Cys-native or Cys$^{57}$- and Cys$^{146}$-replaced mutant SOD1s were co-expressed with Dorfin, ubiquitylation of mutant SOD1s were increased; however, co-expression of Dorfin with mutant SOD1 in which Cys$^6$ and Cys$^{111}$ or all four Cys residues were replaced did not promote ubiquitylation of these mutant SOD1s (Fig. 7*B*). Chase experiments with cycloheximide in the presence or absence of Dorfin demonstrated that degradation of Cys-native and Cys$^{57}$- and Cys$^{146}$-replaced mutant SOD1$^{G93A}$ was greatly accelerated when Dorfin was overexpressed, whereas the stability of Cys$^6$ and Cys$^{111}$ or all four Cys-replaced mutant SOD1G93A were unaffected (Fig. 7*C*). We have previously shown that Dorfin exerts neuroprotective effects by promoting degradation of mutant SOD1 through its ubiquityl ligase activities (20). Co-expression of Dorfin improved the viability of Neuro-2a cells expressing Cys-

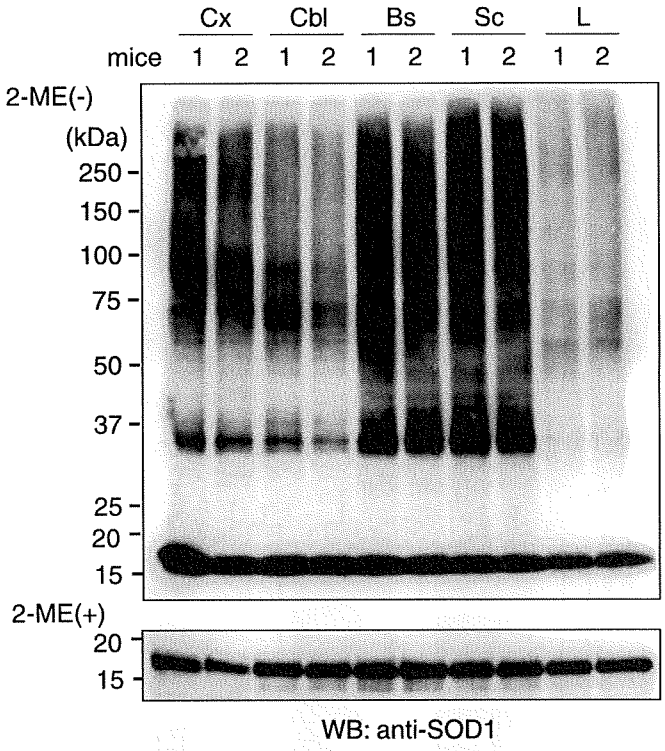


FIGURE 5. **Preferential occurrence of disulfide-cross-linked mutant SOD1 in the affected lesion of ALS model mice.** Western blotting of tissue samples from two 17-week-old symptomatic G93A mutant SOD1-transgenic mice under non-reducing (*upper panel*) and reducing (*lower panel*) conditions. *Cx*, cerebral cortex; *Cbl*, cerebellum; *Bs*, brain stem; *Sc*, spinal cord; *L*, liver.

native and $Cys^{57}$- and $Cys^{146}$-replaced mutant $SOD1^{G93A}$ (Fig. 7*D*).

## DISCUSSION

Mutations in the *SOD1* gene cause familial ALS through the gain of a toxic function, however, the nature of this toxic function remains largely unknown (31). Ubiquitylated aggregates of mutant SOD1 proteins in affected lesions are a pathological hallmark of the disease (32) and suggest their relation to neurotoxicity. Recent biochemical studies suggest that the immature disulfide-reduced forms of the familial ALS mutant SOD1 proteins play a critical role in this neurotoxicity; *in vitro*, these forms tend to misfold, oligomerize, and readily undergo incorrect disulfide bond formation upon mild oxidative stress (16, 33). Among the more than 100 ALS-associated human SOD1 mutants, some cannot intrinsically form the essential intramolecular disulfide bonds. One of the conserved Cys residues, $Cys^{146}$, is missing in some of the mutants, such as the $Leu^{126}$ del TT (stop at 131) and $Gly^{127}$ ins TGGG (stop at 133); however, it has been reported that minute quantities of SOD1 aggregates can cause the disease in mice expressing the truncated mutant, $Gly^{127}$ ins TGGG (stop at 133) (34). Furthermore, a significant fraction of the insoluble SOD1 aggregates in the spinal cord of ALS model mice contain multimers cross-linked via intermolecular disulfide bonds (17, 35). In the present study, we showed that non-physiological intermolecular disulfide bonds involving $Cys^{6}$ and $Cys^{111}$ of the mutant SOD1 were important for high molecular weight aggregate formation, ubiquitylation, and neurotoxicity *in vivo*, all of which were dramatically reduced in Neuro-2a cells when these residues were replaced with serines.

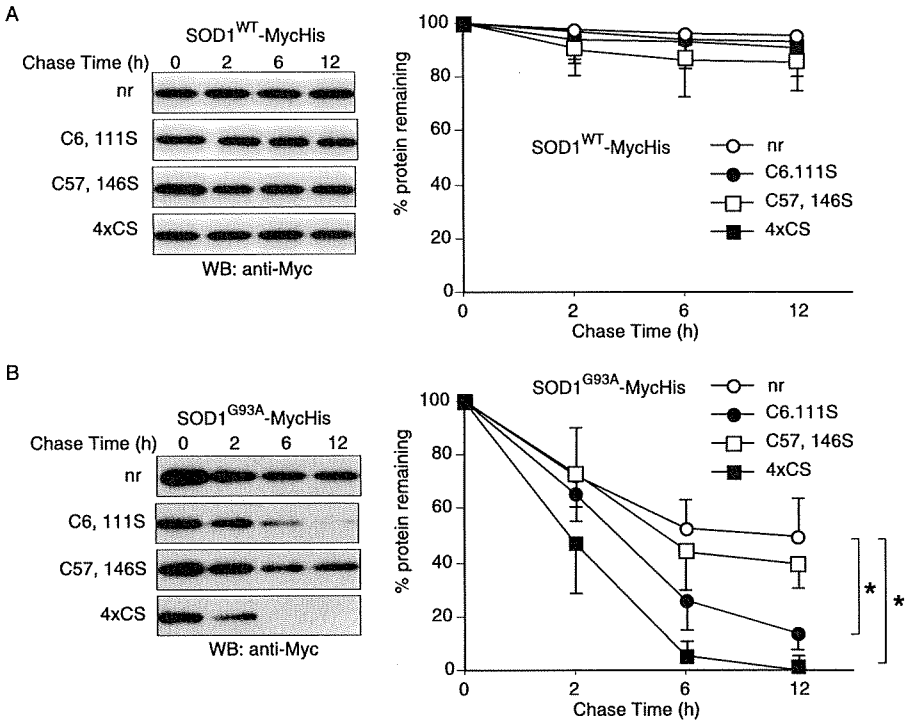


FIGURE 6. **Effects of disulfide-linking at $Cys^{6}$ and $Cys^{111}$ on the rate of mutant SOD1 degradation.** Cycloheximide chase analysis on Neuro-2a cells expressing (*A*) wild-type (*WT*) and (*B*) G93A mutant SOD1 and their Cys to Ser derivatives. Western blots showing levels of SOD1 protein at various times after the cycloheximide chase are in the *left panels*. Quantitative data on the right are mean ± S.D. values of three independent experiments. Statistical analyses were carried out by analysis of variance. *, $p < 0.01$. *nr*, SOD1 without cysteine residue replacement; *4×CS*, all four cysteines replaced by serines.

Human SOD1 has two free cysteine residues, $Cys^{6}$ and $Cys^{111}$ (36). $Cys^{6}$ is located adjacent to the dimer interface pointed toward the interior of the β-barrel and is solute-inaccessible in the native, folded conformation. $Cys^{111}$ is located near the surface and is solute-accessible and -reactive, often becoming blocked during purification (37). Replacement of the free Cys residues increased the resistance to thermal inactivation (38). Increased resistance of mutant SOD1s is due to increased resistance to irreversible unfolding and relatively unaffected by changes in conformational stability (39). Our data, showing that aggregate formation of mutant SOD1 is reduced when $Cys^{6}$ and $Cys^{111}$ are replaced with serines, are compatible with these observations. Mutations of the $Cys^{6}$ residue (C6F and C6G) still result in familial ALS (4), and in a transgenic mouse expressing mouse SOD1 retaining cystines 6, 57, and 146 but lacking

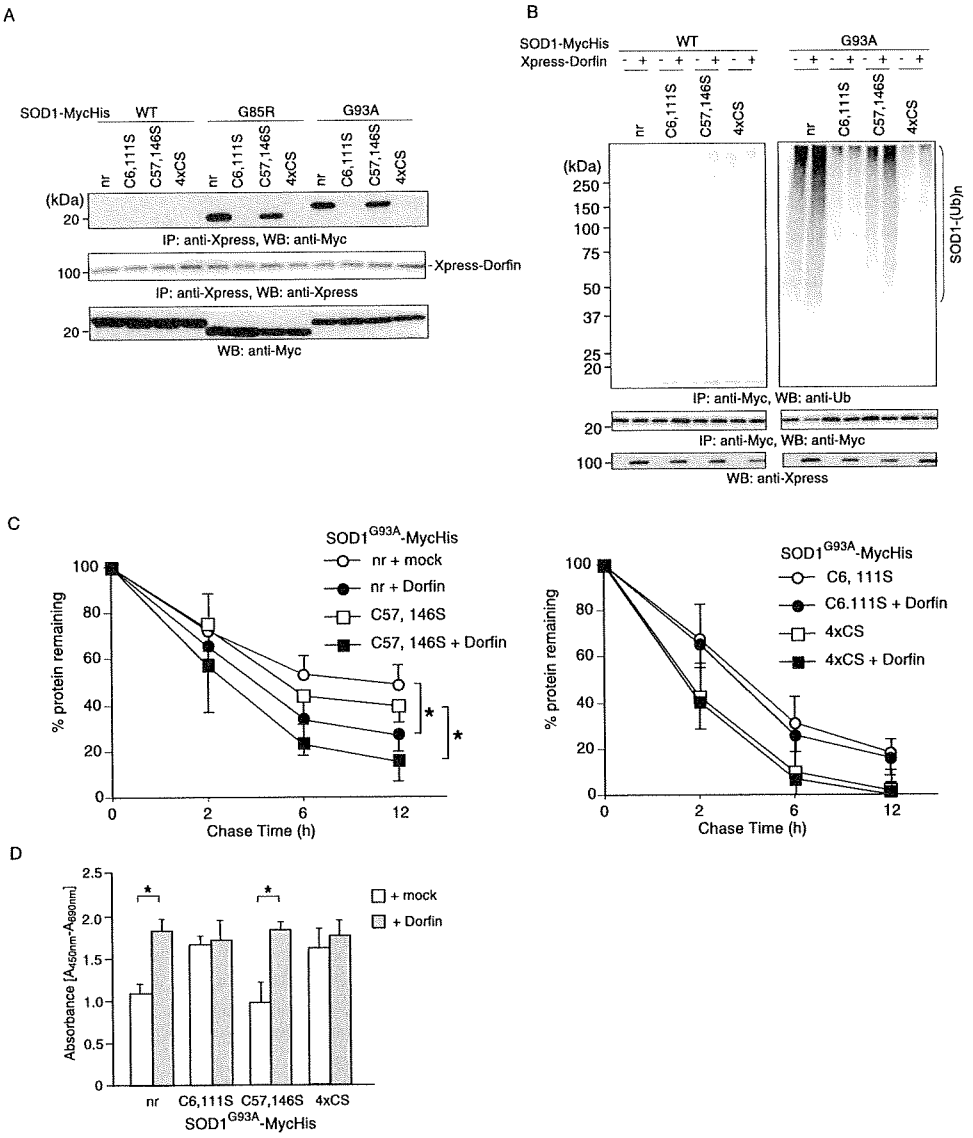


FIGURE 7. **Ubiquityl ligase Dorfin binds, ubiquitylates, and promotes degradation of disulfide-linked mutant SOD1.** *A*, replacement of $Cys^6$ and $Cys^{111}$ nearly eliminated the interaction of Dorfin with mutant SOD1. Various SOD1-MycHis were co-transfected with Xpress-Dorfin. After immunoprecipitation with anti-Xpress antibody, the resulting precipitates and cell lysates were analyzed by Western blotting with anti-Myc antibody. *B, in vivo*, Dorfin failed to promote ubiquitylation of mutant SOD1 with the $Cys^6$ and $Cys^{111}$ replacement. Western blotting of SOD1-Myc-His immunoprecipitates with anti-ubiquitin antibody. *C*, Dorfin failed to promote degradation of mutant SOD1 with both $Cys^6$ and $Cys^{111}$ replaced. Cycloheximide chase analysis of G93A mutant SOD1 with $Cys^6$ and $Cys^{111}$-replacements (*left panel*) or with $Cys^{57}$ and $Cys^{146}$-replacements (*right panel*) in the presence or absence of overexpressed Xpress-Dorfin. *D*, Dorfin prevented neurotoxicity by mutant SOD1 with intact $Cys^6$ and $Cys^{111}$ residues. Cell viability was measured by the WST-1-based assay. Data are mean ± S.D. values of three independent experiments. Statistical analyses were carried out by unpaired *t* test. *, $p < 0.01$. *nr*, SOD1 without replacement in cysteine residue; *4×CS*, all four cysteines replaced by serines.

111 and with a G86R mutation corresponding to G85R mutation in human SOD1, degeneration of motor neurons in the spinal cord has been observed (40). These results imply that, if one of either the $Cys^6$ or $Cys^{111}$ residues is present, it can still be a disease-causing SOD1. Our data here also revealed that replacement of only one of the Cys residues at positions 6 or 111 had modest effects on the formation of aggregates (Fig. 2).

Cytoplasmic proteins are degraded mainly via two pathways, the ubiquitin-proteasome pathway (6) and via autophagy (7). Previous studies have shown that mutant SOD1 proteins are turned over more rapidly than wild-type SOD1 (12, 18, 19). Two distinct ubiquitin ligases, Dorfin and NEDL1, were reported to specifically ubiquitylate mutant but not wild-type SOD1 (20, 21). These studies suggest that mutant SOD1 is degraded by the ubiquitin-proteasome pathway and that the accelerated turnover of mutant SOD1 is mediated in part by this pathway. Impairment of the proteasome activities may contribute to ALS pathogenesis (28, 41, 42). We showed here that proteasome inhibition led to a dose-dependent accumulation of aberrant disulfide-linked high molecular weight mutant SOD1 (Fig. 1), suggesting that disulfide-linking mediates ubiquitylation of mutant SOD1. In fact, we found that Dorfin ubiquitylated mutant SOD1 by recognizing the $Cys^6$ and $Cys^{111}$ disulfide cross-linked form and targeted it for proteasomal degradation (Fig. 7). Mutant SOD1, in which the $Cys^6$ and $Cys^{111}$ were replaced, was not ubiquitylated (Fig. 3), and its rate of degradation was not affected in the presence of Dorfin (Fig. 7). It is possible that mutant SOD1 lacking $Cys^6$ and $Cys^{111}$ may be degraded directly by the proteasome without ubiquitylation (43) or by autophagy (44), but further studies are needed to address this issue.

The appearance of mutant SOD1 aggregates in motor neurons of familial ALS patients and mouse models has suggested that aggregation plays an important role in neurotoxicity (31). However, conflicting results have been reported on the correlation between aggregate formation and cell death. One report showed that aggregate formation of mutant $SOD1^{A4V}$ and $SOD1^{V148G}$ does not correlate with cell death (45), whereas another study using live cell-imaging techniques reported that the ability of mutant $SOD1^{G85R}$ and $SOD1^{G93A}$ proteins to form aggregates directly correlates with neuronal cell death (46). These controversies also exist in other neurodegenerative diseases (47, 48). In this study, we clearly showed a direct link among intermolecular disulfide bond-mediated high molecular weight complex formation, visible aggregate formation, and neurotoxicity (Figs. 2–4).

Furukawa *et al.* (16) reported that formation of disulfide-linked multimers need not involve the non-conserved Cys residues, $Cys^6$ and $Cys^{111}$, and that the conserved Cys residues, $Cys^{57}$ and $Cys^{146}$, play an important role in the apo-form of

SOD1 multimerization upon oxidative stress. Our results underscore the importance of $Cys^{6}$ and $Cys^{111}$ for high molecular weight aggregate formation, ubiquitylation, and neurotoxicity in Neuro-2a cells. This discrepancy may result from differences in experimental conditions; we studied human SOD1 proteins expressed in Neuro-2a cells, and Furukawa *et al.* used the purified apo-form of human SOD1 from *Escherichia coli*. Further studies will clarify the roles of each of the Cys residues of the mutant SOD1 protein in the ALS pathogenesis *in vivo* by generating transgenic mice bearing mutant SOD1 lacking $Cys^{6}$ and $Cys^{111}$ or $Cys^{57}$ and $Cys^{146}$.

## REFERENCES


1. McCord, J. M., and Fridovich, I. (1969) *J. Biol. Chem.* **244,** 6049–6055
2. Fridovich, I. (1974) *Adv. Enzymol. Relat. Areas. Mol. Biol.* **41,** 35–97
3. Rosen, D. R. (1993) *Nature* **364,** 362
4. Valentine, J. S., Doucette, P. A., and Potter, S. Z. (2005) *Annu. Rev. Biochem.* **74,** 563–593
5. Crapo, J. D., Oury, T., Rabouille, C., Slot, J. W., and Chang, L. Y. (1992) *Proc. Natl. Acad. Sci. U. S. A.* **89,** 10405–10409
6. Fridovich, I. (1986) *Adv. Enzymol. Relat. Areas. Mol. Biol.* **58,** 61–97
7. Fisher, C. L., Cabelli, D. E., Tainer, J. A., Hallewell, R. A., and Getzoff, E. D. (1994) *Proteins* **19,** 24–34
8. Arnesano, F., Banci, L., Bertini, I., Martinelli, M., Furukawa, Y., and O'Halloran, T. V. (2004) *J. Biol. Chem.* **279,** 47998–48003
9. Freedman, R. B. (1995) *Curr. Opin. Struct. Biol.* **5,** 85–91
10. Lindenau, J., Noack, H., Possel, H., Asayama, K., and Wolf, G. (2000) *Glia* **29,** 25–34
11. Tiwari, A., and Hayward, L. J. (2003) *J. Biol. Chem.* **278,** 5984–5992
12. Borchelt, D. R., Lee, M. K., Slunt, H. S., Guarnieri, M., Xu, Z. S., Wong, P. C., Brown, R. H., Jr., Price, D. L., Sisodia, S. S., and Cleveland, D. W. (1994) *Proc. Natl. Acad. Sci. U. S. A.* **91,** 8292–8296
13. Ratovitski, T., Corson, L. B., Strain, J., Wong, P., Cleveland, D. W., Culotta, V. C., and Borchelt, D. R. (1999) *Hum. Mol. Genet* **8,** 1451–1460
14. Rakhit, R., Crow, J. P., Lepock, J. R., Kondejewski, L. H., Cashman, N. R., and Chakrabartty, A. (2004) *J. Biol. Chem.* **279,** 15499–15504
15. Doucette, P. A., Whitson, L. J., Cao, X., Schirf, V., Demeler, B., Valentine, J. S., Hansen, J. C., and Hart, P. J. (2004) *J. Biol. Chem.* **279,** 54558–54566
16. Furukawa, Y., and O'Halloran, T. V. (2005) *J. Biol. Chem.* **280,** 17266–17274
17. Furukawa, Y., Fu, R., Deng, H. X., Siddique, T., and O'Halloran, T. V. (2006) *Proc. Natl. Acad. Sci. U. S. A.* **103,** 7148–7153
18. Hoffman, E. K., Wilcox, H. M., Scott, R. W., and Siman, R. (1996) *J. Neurol. Sci.* **139,** 15–20
19. Johnston, J. A., Dalton, M. J., Gurney, M. E., and Kopito, R. R. (2000) *Proc. Natl. Acad. Sci. U. S. A.* **97,** 12571–12576
20. Niwa, J., Ishigaki, S., Hishikawa, N., Yamamoto, M., Doyu, M., Murata, S., Tanaka, K., Taniguchi, N., and Sobue, G. (2002) *J. Biol. Chem.* **277,** 36793–36798
21. Miyazaki, K., Fujita, T., Ozaki, T., Kato, C., Kurose, Y., Sakamoto, M., Kato, S., Goto, T., Itoyama, Y., Aoki, M., and Nakagawara, A. (2004) *J. Biol. Chem.* **279,** 11327–11335
22. Niwa, J., Ishigaki, S., Doyu, M., Suzuki, T., Tanaka, K., and Sobue, G. (2001) *Biochem. Biophys. Res. Commun.* **281,** 706–713
23. Marin, I., and Ferrus, A. (2002) *Mol. Biol. Evol.* **19,** 2039–2050
24. Lee, H. J., and Lee, S. J. (2002) *J. Biol. Chem.* **277,** 48976–48983
25. Scherzinger, E., Lurz, R., Turmaine, M., Mangiarini, L., Hollenbach, B., Hasenbank, R., Bates, G. P., Davies, S. W., Lehrach, H., and Wanker, E. E. (1997) *Cell* **90,** 549–558
26. Bailey, C. K., Andriola, I. F., Kampinga, H. H., and Merry, D. E. (2002) *Hum. Mol. Genet.* **11,** 515–523
27. Wang, J., Xu, G., and Borchelt, D. R. (2002) *Neurobiol. Dis.* **9,** 139–148
28. Urushitani, M., Kurisu, J., Tsukita, K., and Takahashi, R. (2002) *J. Neurochem.* **83,** 1030–1042
29. Gurney, M. E., Pu, H., Chiu, A. Y., Dal Canto, M. C., Polchow, C. Y., Alexander, D. D., Caliendo, J., Hentati, A., Kwon, Y. W., Deng, H. X., Chen, W., Zhai, P., Sufit, R. L., and Siddique, T. (1994) *Science* **264,** 1772–1775
30. Bruijn, L. I., Houseweart, M. K., Kato, S., Anderson, K. L., Anderson, S. D., Ohama, E., Reaume, A. G., Scott, R. W., and Cleveland, D. W. (1998) *Science* **281,** 1851–1854
31. Cleveland, D. W., and Rothstein, J. D. (2001) *Nat. Rev. Neurosci.* **2,** 806–819
32. Watanabe, M., Dykes-Hoberg, M., Culotta, V. C., Price, D. L., Wong, P. C., and Rothstein, J. D. (2001) *Neurobiol. Dis.* **8,** 933–941
33. Wang, J., Xu, G., and Borchelt, D. R. (2006) *J. Neurochem.* **96,** 1277–1288
34. Jonsson, P. A., Graffmo, K. S., Andersen, P. M., Brannstrom, T., Lindberg, M., Oliveberg, M., and Marklund, S. L. (2006) *Brain* **129,** 451–464
35. Deng, H. X., Shi, Y., Furukawa, Y., Zhai, H., Fu, R., Liu, E., Gorrie, G. H., Khan, M. S., Hung, W. Y., Bigio, E. H., Lukas, T., Dal Canto, M. C., O'Halloran, T. V., and Siddique, T. (2006) *Proc. Natl. Acad. Sci. U. S. A.* **103,** 7142–7147
36. Getzoff, E. D., Tainer, J. A., Stempien, M. M., Bell, G. I., and Hallewell, R. A. (1989) *Proteins* **5,** 322–336
37. Briggs, R. G., and Fee, J. A. (1978) *Biochim. Biophys. Acta* **537,** 86–99
38. McRee, D. E., Redford, S. M., Getzoff, E. D., Lepock, J. R., Hallewell, R. A., and Tainer, J. A. (1990) *J. Biol. Chem.* **265,** 14234–14241
39. Lepock, J. R., Frey, H. E., and Hallewell, R. A. (1990) *J. Biol. Chem.* **265,** 21612–21618
40. Ripps, M. E., Huntley, G. W., Hof, P. R., Morrison, J. H., and Gordon, J. W. (1995) *Proc. Natl. Acad. Sci. U. S. A.* **92,** 689–693
41. Kabashi, E., Agar, J. N., Taylor, D. M., Minotti, S., and Durham, H. D. (2004) *J. Neurochem.* **89,** 1325–1335
42. Cheroni, C., Peviani, M., Cascio, P., Debiasi, S., Monti, C., and Bendotti, C. (2005) *Neurobiol. Dis.* **18,** 509–522
43. Di Noto, L., Whitson, L. J., Cao, X., Hart, P. J., and Levine, R. L. (2005) *J. Biol. Chem.* **280,** 39907–39913
44. Kabuta, T., Suzuki, Y., and Wada, K. (2006) *J. Biol. Chem.* **281,** 30524–30533
45. Lee, J. P., Gerin, C., Bindokas, V. P., Miller, R., Ghadge, G., and Roos, R. P. (2002) *J. Neurochem.* **82,** 1229–1238
46. Matsumoto, G., Stojanovic, A., Holmberg, C. I., Kim, S., and Morimoto, R. I. (2005) *J. Cell Biol.* **171,** 75–85
47. Arrasate, M., Mitra, S., Schweitzer, E. S., Segal, M. R., and Finkbeiner, S. (2004) *Nature* **431,** 805–810
48. Saudou, F., Finkbeiner, S., Devys, D., and Greenberg, M. E. (1998) *Cell* **95,** 55–66

J Neuropathol Exp Neurol

Vol. 66, No. 7
July 2007
pp. 617–627

ORIGINAL ARTICLE

# Gene Expressions Specifically Detected in Motor Neurons (Dynactin 1, Early Growth Response 3, Acetyl-CoA Transporter, Death Receptor 5, and Cyclin C) Differentially Correlate to Pathologic Markers in Sporadic Amyotrophic Lateral Sclerosis

Yue-Mei Jiang, PhD, Masahiko Yamamoto, MD, Fumiaki Tanaka, MD, Shinsuke Ishigaki, MD, Masahisa Katsuno, MD, Hiroaki Adachi, MD, Jun-ichi Niwa, MD, Manabu Doyu, MD, Mari Yoshida, MD, Yoshio Hashizume, MD, and Gen Sobue, MD

**Abstract**

In a differential gene expression profile, we showed previously that dynactin 1 (*DCTN1*), early growth response 3 (*EGR3*), acetyl-CoA transporter (*ACATN*), death receptor 5 (*DR5*), and cyclin C (*CCNC*) were prominently up- or downregulated in motor neurons of sporadic amyotrophic lateral sclerosis (ALS). In the present study, we examined the correlation between the expression levels of these genes and the levels of pathologic markers for motor neuron degeneration (i.e. cytoplasmic accumulation of phosphorylated neurofilament H [pNF-H] and ubiquitylated protein) and the numbers of residual motor neurons in 20 autopsies of patients with sporadic ALS. *DCTN1* and *EGR3* were widely downregulated, and the changes in gene expression were correlated to the number of residual motor neurons. In particular, *DCTN1* was markedly downregulated in most residual motor neurons before the accumulation of pNF-H, even in cases with well-preserved motor neuron populations. *ACATN*, *DR5*, and *CCNC* were upregulated in subpopulations of residual motor neurons, and their expression levels were well correlated with the levels of pNF-H accumulation and the number of residual motor neurons. The expressions of *DCTN1*, *EGR3*, *ACATN*, and *DR5* were all markedly altered before ubiquitylated protein accumulation. *DCTN1* downregulation appears to be an early event before the appearance of neurodegeneration markers, whereas upregulations of *DR5* and *CCNC* are relatively later phenomena associated with pathologic markers and leading to neuronal death. The sequence of motor neuron-specific gene expression changes in sporadic ALS can be beneficial information in developing appropriate therapeutic strategies for neurodegeneration.

**Key Words:** Amyotrophic lateral sclerosis (ALS), Axonal transport, Cell death, Dynactin 1, Motor neuron.

## INTRODUCTION

Amyotrophic lateral sclerosis (ALS) is a devastating neurodegenerative disease characterized by loss of motor neurons in the spinal cord, brainstem, and motor cortex (1), causing weakness of the limbs, abnormalities of speech, and difficulties in swallowing. The weakness ultimately progresses to respiratory impairment and half of the patients die within 3 years of the onset of symptoms, largely due to respiratory failure. About 5% to 10% of all patients with ALS show familial traits, and 20% to 30% of patients with familial ALS have a mutation in the copper/zinc superoxide dismutase 1 gene (*SOD1*). However, in more than 90% of patients with ALS, the disease is sporadic and does not show any familial traits. The presence of Bunina bodies in the remaining spinal motor neurons is a hallmark of cases of sporadic ALS (2, 3). There is at present no obvious consensus understanding of the pathogenic mechanism or an effective therapeutic approach for sporadic ALS, although several hypotheses, including oxidative stress, glutamate excitotoxicity, impaired axonal transport, neurofilament disintegration, mitochondrial dysfunction, neurotrophic deprivation, and proteasomal dysfunction have been proposed as causal mechanisms of motor neuron degeneration (4–11). In contrast, wide-ranging research activities have been initiated for a subgroup of patients with familial ALS, those with mutant *SOD1*, including a search for the pathogenic mechanisms of mutant SOD1-induced motor neuron death and the examination of therapeutic perspectives using a transgenic rodent model for mutant SOD1 familial ALS (12–14).

One effective approach to begin the uncovering of the pathogenic mechanism of sporadic ALS is a description of

From the Department of Neurology (Y-MJ, MY, FT, SI, MK, HA, J-IN, MD, GS), Nagoya University Graduate School of Medicine, Nagoya, Japan; Department of Speech Pathology and Audiology (MY), Aichi Gaguin University School of Health Science, Nisshin, Aichi, Japan; and Department of Neuropathology (MY, YH), Institute for Medical Science of Aging, Aichi Medical University School of Medicine, Nagakute, Aichi, Japan.

Drs. Jiang and Yamamoto contributed equally to this work.

Send correspondence and reprint requests to: Dr. Gen Sobue, Department of Neurology, Nagoya University Graduate School of Medicine, Nagoya 466-8550, Japan; E-mail: sobueg@med.nagoya-u.ac.jp

This work was supported by the 21st Century COE Program "Integrated Molecular Medicine for Neuronal and Neoplastic Disorders" from the Ministry of Education, Culture, Sports, Science and Technology of Japan, and grants from the Ministry of Health, Labor and Welfare of Japan.

the gene expression profile of motor neurons. Motor neuron-specific gene expression profiling would eventually lead us to a profound understanding of the pathophysiology of motor neuron degeneration in sporadic ALS. We have successfully created such a motor neuron-specific gene expression profile in patients with sporadic ALS by using microarray technology combined with laser-captured microdissection, the results of which were further verified by in situ hybridization and quantitative wide-ranging research activities (15). The genes with differential expressions in these profiles were particularly related to axonal transport, transcription, energy production, cell death, and protection from cell death. Gene expressions of dynactin 1 (*DCTN1*) and early growth response 3 (*EGR3*), related to cytoskeleton/axonal transport and transcription, respectively, were markedly decreased in motor neurons, whereas cell death-associated genes such as death receptor 5 (*DR5*), cyclin C (*CCNC*), and acetyl-CoA transporter (*ACATN*) were greatly upregulated. It is, however, uncertain how these gene expression alterations correlate with motor neuron degeneration and death and whether they play a role in the pathogenesis of sporadic ALS. A description of the molecular events underlying motor neuron degeneration in sporadic ALS, even particular short aspects of a long sequence of the degeneration process, would provide a beneficial therapeutic avenue for sporadic ALS by enabling development of a disease model simulating these molecular events.

In this study we further characterized the gene expression profiles of *DCTN1*, *EGR3*, *ACATN*, *DR5*, and *CCNC* in individual motor neurons and compared their expression levels with those of known motor neuron neurodegeneration markers, cytoplasmic accumulations of phosphorylated neurofilament H (pNF-H), ubiquitylated proteins, and with neuronal loss (5, 16–18). We found that changes in expression levels of these genes differentially reflect the motor neuron degeneration process, and, in particular, *DCTN1* is extensively downregulated before the appearance of these degeneration markers.

## MATERIALS AND METHODS

### Tissues From Patients with Amyotrophic Lateral Sclerosis and Control Patients

Specimens of lumbar spinal cord (L4–L5 segments) from 20 patients with sporadic ALS (11 male and 9 female) and 8 neurologically normal patients (4 male and 4 female) as controls were obtained at autopsy. The diagnosis of ALS was confirmed by El Escorial diagnostic criteria defined by the World Federation of Neurology and by histopathologic findings, particularly the presence of Bunina bodies (2, 3). All patients with ALS had sporadic ALS and showed no hereditary traits. Patients with a *SOD1* mutation were excluded. The collection of tissues and their use for this study were approved by the ethics committee of Nagoya University Graduate School of Medicine. The ages for patients with ALS and control patients were 63.3 ± 11.5 (mean ± SD) (range 43–80) and 65.4 ± 12.7 (42–79) years, respectively, and the ALS illness duration was 2.9 ± 0.87 (1.2–4.3) years. The postmortem intervals to autopsy for patients with ALS and control patients were 7.3 ± 3.9 (3–15) and 8.6 ± 3.2 (4–13) hours, respectively. There were no significant differences in either age or postmortem interval between the ALS and control groups. Among 20 patients, severe bulbar symptoms were seen in 14 cases, severe upper limb wasting in 17 cases, and severe lower limb wasting in 13 cases in the advanced stage. The upper motor neuron signs were seen in 13 patients, whereas others showed predominantly lower motor neuron signs. Most of the patients with ALS developed respiratory dysfunction in various degrees, with eventually resulted in respiratory failure in all patients, which was the cause of death. The cause of death in the control patients was pneumonia, cancer, stroke, or acute heart attack. Tissues were immediately frozen in liquid nitrogen and stored at −80°C until use. Parts of the lumbar spinal cord were fixed in 10% buffered formalin solution and processed for paraffin sections. The sections were stained with hematoxylin and eosin and Klüver-Barrera techniques and further histologic assessments were performed.

### Selection of Genes Examined Based on Our Previous Microarray Analysis in Laser-Captured Motor Neurons of Patients with Sporadic Amyotrophic Lateral Sclerosis

By using microarray technology combined with laser-captured microdissection, gene expression profiles of degenerating spinal motor neurons isolated from autopsied patients with sporadic ALS were previously reported (15). Three percent of genes examined were downregulated, and 1% were upregulated. We selected 5 genes (*DCTN1* associated with cytoskeleton/axonal transport *EGR3* as a transcription factor, and *ACATN*, *DR5* and *CCNC* as cell death-associated genes), which were most prominently down- or upregulated (15). These changes in gene expression were confirmed by cluster analyses of hierarchical clustering, self-organizing maps, and principal component analyses after logarithmic transformation, as motor neuron-specific gene expression changes distinctive from the spinal ventral horn as a whole, and their alterations were further quantitatively verified by real-time wide-ranging research activities and in situ hybridization. In addition, these 5 genes were chosen for the present study because they cover a wide range and represent different aspects of the functional hierarchy.

### In Situ Hybridization

Frozen, 10-μm-thick spinal cord sections were prepared and immediately fixed in 4% paraformaldehyde. The sections were then treated with 0.1% diethylpyrocarbonate twice for 15 minutes and prehybridized at 45°C for 1 hour. Digoxigenin-labeled cRNA probes were generated from linearized plasmids for the genes of interest using SP6 or T7 polymerase (Roche Diagnostics, Basel, Switzerland). Gene names, GenBank accession numbers, probe positions (nucleotide [nt] number), and probe sizes (base pairs [bp]) were as follows: acetyl-CoA transporter (*ACATN*), D88152, nt 397–741, 345 bp; dynactin 1 (*DCTN1*), NM_004082, nt 2392–2774, 383 bp; death receptor 5 (*DR5*), NM_004082, nt 682–1070, 389 bp; and early growth response 3 (*EGR3*), NM_004430, nt 1433–1794, 362 bp. After prehybridization

the sections were hybridized with digoxigenin-labeled cRNA probes overnight at 45°C. The washed sections were incubated with alkaline phosphatase-conjugated, anti-digoxigenin antibody (Roche Diagnostics). The signal was visualized with nitro blue tetrazolium/5-bromo-4-chloro-3-indolyl phosphate (Roche Diagnostics). No hybridization signal was observed with the sense probe for the expression of each gene in spinal motor neurons.

## Immunohistochemistry

Frozen, 10-μm-thick spinal cord sections were prepared and immediately fixed in 4% paraformaldehyde. The sections were then blocked with 2% bovine serum albumin (Sigma) in Tris-buffered saline at room temperature for 20 minutes and incubated with either a monoclonal antibody against the phosphorylated epitope in the tail domain of neurofilament H (anti-SMI 31, 1:1000; Sternberger Monoclonals Inc., Lutherville, MD), anti-cyclin C antibody (1:200; Santa Cruz Biotechnology, Santa Cruz, CA), or anti-ubiquitin (1:1000; Santa Cruz Biotechnology) overnight at 4°C. Subsequent procedures were carried out using the EnVision+Kit/HRP (DAB) (DAKO, Glostrup, Denmark) according to the manufacturer's protocol.

## Quantitative Assessment of Gene Expression Levels, Population of Residual Motor Neurons, and Cytoplasmic Accumulation of Phosphorylated Neurofilament H and Ubiquitylated Proteins

To assess gene and protein expression levels in spinal motor neurons, signal intensities of in situ hybridization and immunohistochemistry, respectively, were quantified using a CCD image analyzer (Zeiss Axiovert S100TV) as described previously (19, 20). Images of individual motor neurons on transverse sections of spinal cord with signals for *DCTN1*, *EGR3*, *ACATN*, *DR5*, or CCNC and pNF-H were captured at the desired magnification and stored with image software (Adobe Photoshop). Grey-scale levels in 65,536 gradations of the images were quantitatively analyzed with image analysis software (Image Gauge version 4.0, Fujifilm, Tokyo, Japan). Signal intensities were expressed as individual intracellular cytoplasmic signal levels (arbitrary absorbance units/mm$^2$) of motor neuron for each gene of interest by subtracting the mean background levels of 3 regions of interest in each section. We also assessed motor neurons harboring ubiquitylated proteins on the anti-ubiquitin-stained sections. Motor neurons with dot-like accumulations, skein-like accumulations, or large inclusions of cytoplasmic ubiquitylated proteins were designated as positive for ubiquitylated protein accumulation.

To count the number of remaining spinal motor neurons, 10-μm-thick serial sections were prepared from the lumber segment of spinal cords and every 10th section was stained with the Klüver-Barrera technique. The ventral spinal horn was designated as the grey matter ventral to the line through the central spinal canal perpendicular to the ventral spinal sulcus, and the residual motor neuron population was defined as the number of relatively large-sized ventral horn cells of 24.8 μm or more in diameter with distinct nucleoli on 10 sections, as described previously (21). Our previous study demonstrated the neuron loss predominantly in the relatively large neurons in ALS (21).

The frequency of motor neurons showing changes in gene expression levels was assessed in at least 10 transverse sections from each of 20 patients with ALS and 8 control patients. The number of motor neurons with gene expression levels more than ±2 SDs from the control levels was expressed as a percentage of motor neurons. Ten to > 100 motor neurons were examined for each individual case.

To investigate the correlation between gene expression levels and pathologic markers in an individual motor neuron we used consecutive transverse spinal cord sections. Ten sets of consecutive sections for each gene of interest were prepared from each patient and the correlations of gene expression levels with pNF-H accumulation levels and positive or negative ubiquitylated protein accumulations were assessed on individual motor neurons. This assessment was performed for 8 representative patients with ALS and 8 control patients whose sections were available for examination.

## Statistical Analyses

Simple correlation tests were performed to assess the correlation of gene expression levels of *DCTN1*, *EGR3*, *ACATN*, and *DR5* and protein expression of CCNC, with the degree of pNF-H accumulation in individual motor neurons. This test was also applied to assess the correlation of the gene expression changes with the numbers of residual motor neurons. Mann-Whitney U tests were used to compare gene expression levels among the motor neurons that were either positive or negative for ubiquitylated proteins in patients with ALS and in control patients. Significance levels were set to $p < 0.05$.

# RESULTS

## Differential Frequencies of Gene Expression Changes in Residual Motor Neurons: *DCTN1* Is Highly Downregulated

Among the genes examined, *DCTN1* and *EGR3* were downregulated in the vast majority of spinal motor neuron populations in most patients (Fig. 1A, B). In 15 of 20 patients, all of the residual motor neurons had reduced *DCTN1* expression compared with controls (Fig. 1B). Ten of the 20 patients showed downregulation of *EGR3* in all residual neurons (Fig. 1B). *ACATN*, by contrast, was upregulated in all residual motor neurons in only 8 of 20 patients (Fig. 1A, B). *DR5* was upregulated in subpopulations of motor neurons, whereas only 4 patients had upregulated gene expression in all of the residual neurons (Fig. 1A, B). Nuclear accumulation of CCNC protein assessed by immunohistochemistry was observed in only a small percentage of motor neurons in most patients (Fig. 1A, B). There were no patients with CCNC nuclear accumulation in all of the residual neurons (Fig. 1B). Cytoplasmic accumulation of pNF-H was seen in more than half of the residual motor neurons in most of the patients (Fig. 1A). Quantitative assessment showed

that in 9 of the 20 patients, all of the residual motor neurons were positive for pNF-H (Fig. 1B). Thus, the frequency of residual motor neurons with gene up- or downregulation was markedly different depending on the individual gene. This gene-dependent differential gene expression among the residual motor neurons is clearly demonstrated in Figure 1C. Two consecutive transverse sections were subjected to in situ hybridization with different gene probes. *DCTN1*

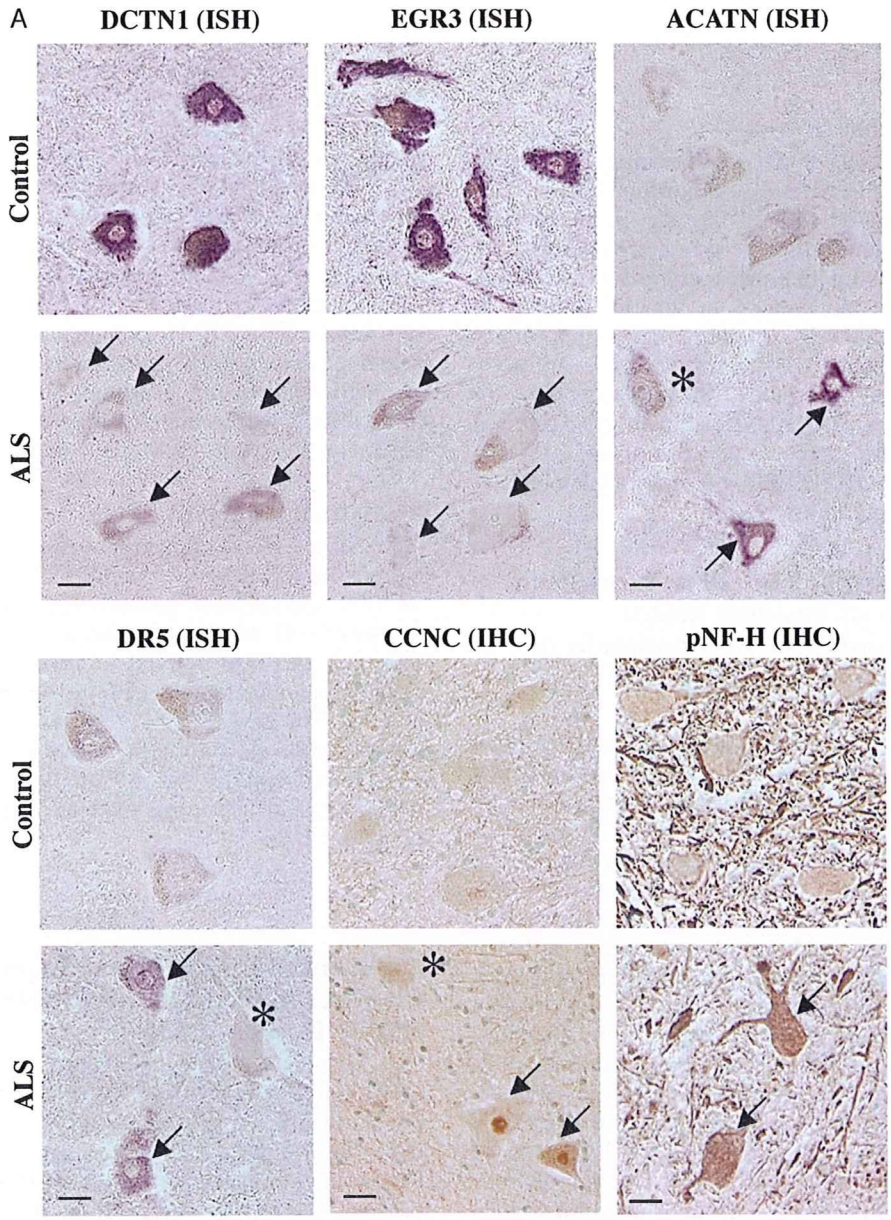


**FIGURE 1.** In situ hybridization (ISH) and immunohistochemistry (IHC) in spinal motor neurons. **(A)** Representative ISHs are shown for dynactin 1 (*DCTN1*), early growth response 3 (*EGR3*), acetyl-CoA transporter (*ACATN*), and death receptor 5 (*DR5*). The antisense probe detects positive signals for the expression of each gene in spinal motor neurons for patients with amyotrophic lateral sclerosis (ALS) and/or control patients, but the sense probe does not (15). RNase treatment before the hybridization abolished the hybridization signals. IHC was performed for cyclin C (CCNC) and phosphorylated neurofilament H (pNF-H). The nuclear staining of CCNC was prominent in ALS motor neurons. Lipofuscin granules are seen as yellowish granules. **(B)** Percentage of motor neurons with gene expression or protein accumulation changes, relative to control levels, among the residual motor neurons in 20 patients with ALS. The quantitative analyses of gene expression and frequency assessments are described in the Materials and Methods section. **(C)** ISH of 2 genes in consecutive sections demonstrates the relationship between up- and downregulated genes in individual motor neurons. *DCTN1* was downregulated to a great extent in all the remaining motor neurons in ALS, whereas *ACATN* and *DR5* were upregulated in only a subpopulation of motor neurons. Arrows denote motor neurons with gene expression changes, and asterisks denote those without changes compared with controls. Scale bars = 25 μm.

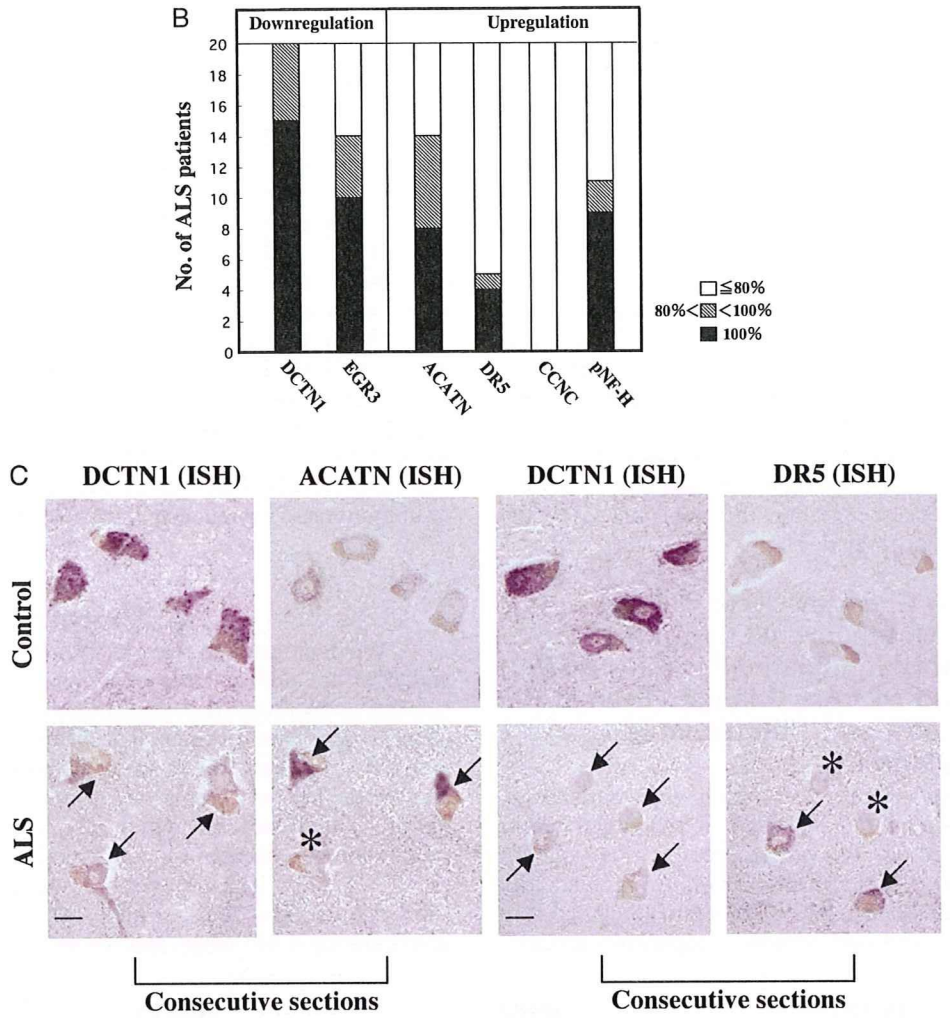


**FIGURE 1.** (continued)

expression was reduced in all the neurons in each panel, whereas some of the residual motor neurons showed unchanged *ACATN* and *DR5* gene expression (Fig. 1C). Moreover, *DCTN1* expression was preserved in neurons other than motor neurons such as those in the dorsal nucleus of Clarke and the intermediolateral nucleus in spinal cords, Purkinje cells of the cerebellum and cortical neurons in the occipital cortex in patients with ALS as well as control patients (data not shown). These findings indicate that, among the genes examined, downregulation of *DCTN1* was specific and extensive in the spinal motor neurons, whereas cell death-related genes such as *ACATN* and *DR5,* and the protein CCNC were upregulated in only subpopulations of motor neurons.

## Gene Expression Changes Are Differentially Correlated With the Population of Residual Motor Neuron: *DCTN1* is Markedly Downregulated Even in Patients With Relatively Well-Preserved Motor Neuron Populations

When the numbers of motor neurons with given gene expression or protein accumulation changes were compared with the numbers of residual motor neurons in the 20 patients, changes in *DR5*, pNF-H, *EGR3*, *ACATN* and *DCTN1* were correlated with the residual motor neuron population ($r = 0.49–0.83$, $p < 0.05$ to 0.0001, Fig. 2). Among them, *DCTN1* expression was most prominently downregulated, even in patients with relatively well-preserved motor neurons, suggesting that *DCTN1* downregulation may be occurring even in early stages of the disease. The changes in expression of *EGR3*, *ACATN*, and *DR5* in patients with well-preserved motor neuron populations were relatively mild compared with that of *DCTN1* (Fig. 2). The change in DR5 expression was less correlated with the residual motor neuron population than that of other genes.

## Gene Expression Changes are Differentially Correlated With the Extent of Motoneuronal Cytoplasmic Phosphorylated Neurofilament H Accumulation: *DCTN1* and *EGR3* Are Markedly Downregulated Before Phosphorylated Neurofilament H Accumulation

The correlation of gene expression and pNF-H accumulation, a marker of neuronal degeneration, in individual motor

neurons was assessed on consecutive sections (Fig. 3A, B). *DCTN1* and *EGR3* downregulations were both marked and independent of the degree of cytoplasmic pNF-H accumulation (Fig. 3B), implying that these genes were widely downregulated even in motor neurons with little or no pNF-H accumulation. By contrast, levels of *ACATN*, *DR5*, and CCNC ranged from just above the control levels to much higher levels and were well correlated with the degree of cytoplasmic pNF-H accumulation ($r = 0.48–0.60$, $p < 0.001$ to 0.0001, Fig. 3B).

These observations indicate that downregulation of *DCTN1* and *EGR3* occurs before the appearance of the neurodegeneration marker pNF-H and thus is a relatively early event in the neurodegeneration process. In contrast, the changes in *ACATN* and *DR5* expression were milder than those in *DCTN1* and *EGR3*, but proportional to pNF-H accumulation, suggesting that their upregulation is a relatively late event, occurring after the appearance of the neurodegeneration marker pNF-H.

### Gene Expression Changes Occur Before Appearance of Motoneuronal Cytoplasmic Accumulation of Ubiquitylated Proteins: *DCTN1*, *EGR3*, *ACATN* and *DR5* Are Changed Even in the Motor Neurons Without Ubiquitylated Protein Accumulation

The correlation of gene expression with cytoplasmic accumulation of ubiquitylated protein in individual motor neurons was assessed on consecutive sections (Fig. 4A, B). In patients with ALS, *DCTN1* and *EGR3* were markedly downregulated, and *ACATN* and *DR5* were upregulated in motor neurons both with and without cytoplasmic accumulation of ubiquitylated proteins (Fig. 4B). However, the degree of downregulation or upregulation was significantly greater in the motor neurons with ubiquitylated protein accumulation compared with those without (Fig. 4B), suggesting that cytoplasmic accumulation of ubiquitylated proteins may be partially correlated to expression changes of *DCTN1*, *EGR3*, and *ACATN*. However, because the expression of these genes changed markedly even in the motor neurons without ubiquitylated proteins, it would imply that cytoplasmic ubiquitylated protein accumulation is a rather late event in the process of motor neuron degeneration.

We further examined the correlation between these 4 gene expression levels and subgroups of motor neurons with 3 different types of ubiquitylated protein accumulation (i.e. dot-like accumulations, skein-like accumulations, and large round inclusions of ubiquitylated proteins), and found that the expression levels of all 4 genes were changed before all types of ubiquitylated protein accumulation (data not shown).

## DISCUSSION

We demonstrated that *DCTN1*, *EGR3*, *ACATN*, *CCNC*, and *DR5* are differentially expressed in the residual motor neurons in sporadic ALS. Furthermore, the expression levels of these genes are differentially correlated with the levels of pathologic markers, the numbers of residual motor neurons, and the degrees of cytoplasmic accumulation of pNF-H and ubiquitylated protein, which are considered to reflect degeneration processes of motor neurons in sporadic ALS (5, 16–18, 22). These 5 genes were selected from those showing the most marked and specific altered expression levels among 4,845 genes that we had previously assessed in

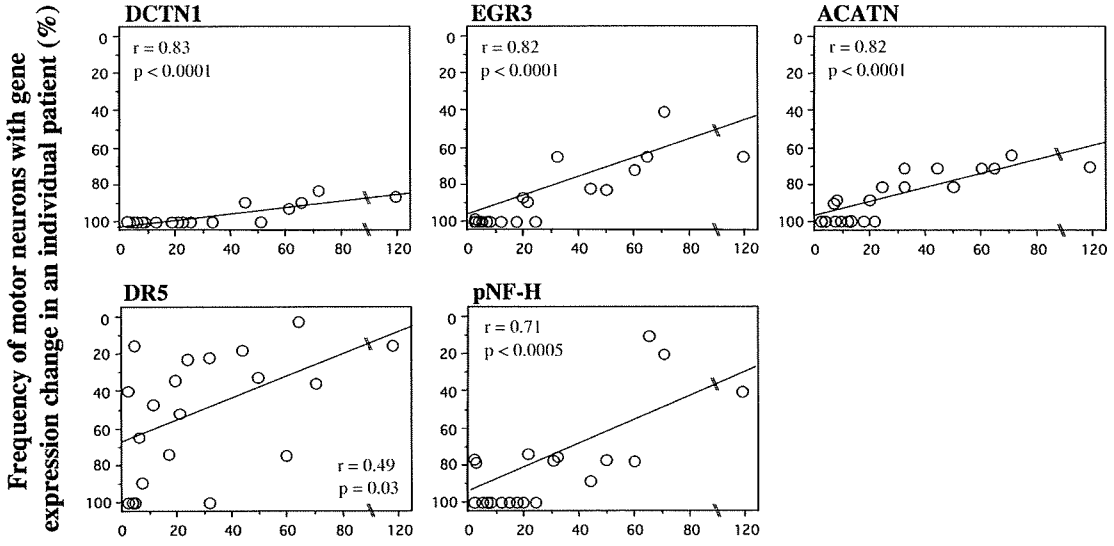


**FIGURE 2.** Frequency of motor neurons with gene expression change correlates with the extent of motor neuron loss. The correlation analyses between frequencies of motor neurons with gene expression changes (relative to controls) for *DCTN1*, *EGR3*, *ACATN*, *DR5*, and pNF-H and numbers of residual motor neurons were performed in the 20 patients with amyotrophic lateral sclerosis. The mean number of motor neuron patients in controls was 195 ± 17 (± SD) (range 176–225)/10 sections (n = 8). The values are inversely ordered on the y axis.

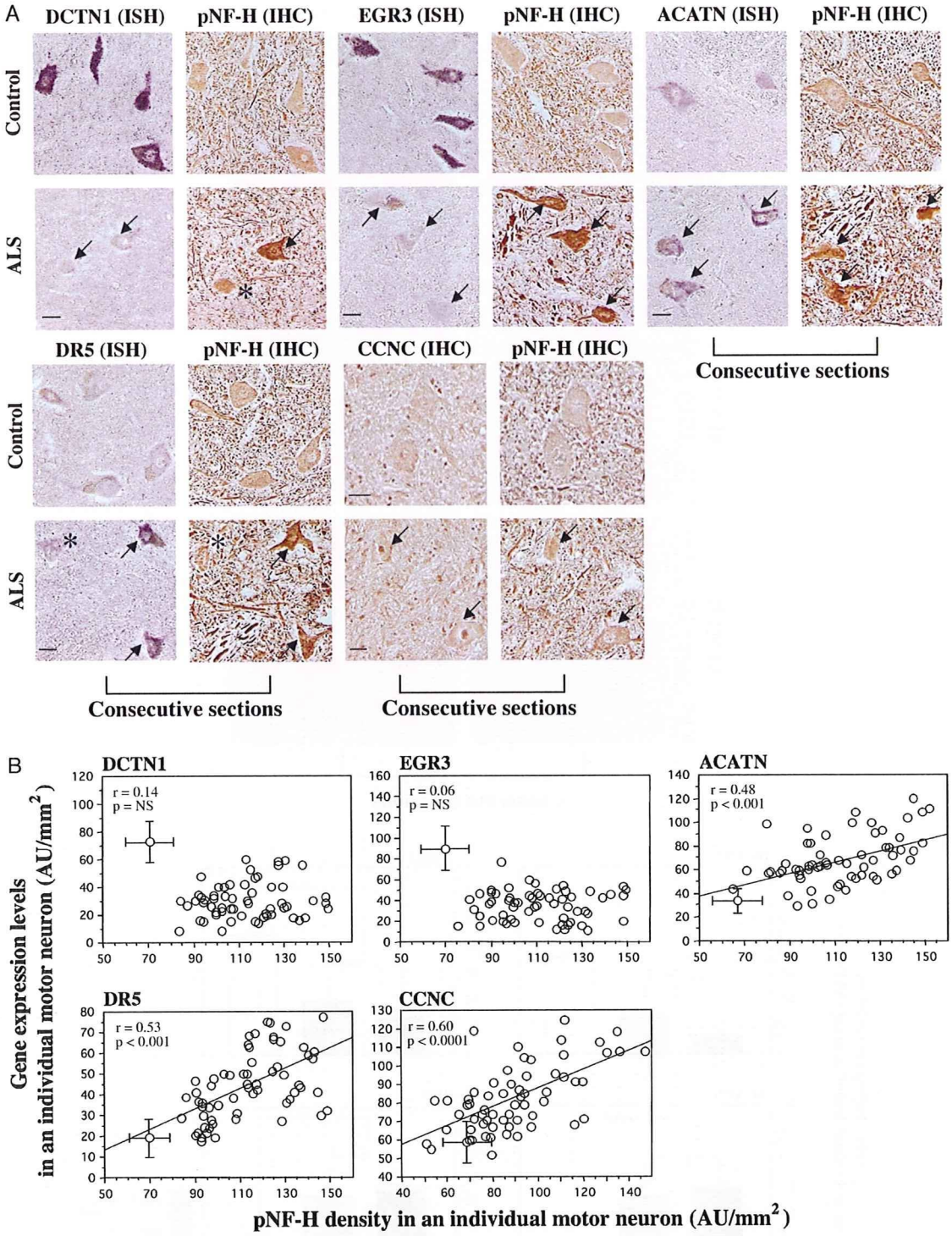


**FIGURE 3.** Gene expression and cytoplasmic phosphorylated neurofilament H (pNF-H) accumulation. **(A)** Gene expressions and pNF-H accumulation in identical motor neurons. Representative in situ hybridization (ISH) for *DCTN1*, *EGR3*, *ACATN*, and *DR5*, and immunohistochemistry (IHC) for CCNC are shown compared with pNF-H staining (IHC) on consecutive spinal cord sections from patients with amyotrophic lateral sclerosis (ALS) and control patients. The accumulation of cytoplasmic pNF-H was prominent in ALS motor neurons. Arrows denote motor neurons with gene expression or protein accumulation changes compared with control patients, and asterisks denote those with unchanged levels. Scale bars = 25 μm. **(B)** Expression levels of genes were compared with the level of pNF-H accumulation in individual motor neurons. Expression levels of *ACATN*, *DR5*, and CCNC were correlated with the accumulation of pNF-H, whereas those of *DCTN1* and *EGR3* were not. Consecutive transverse spinal cord sections were assessed from 8 representative patients with ALS. The control values for gene and protein expression levels and the accumulation of pNF-H are shown as means ± SD for 8 control cases. AU, arbitrary absorbance units; NS, not significant.

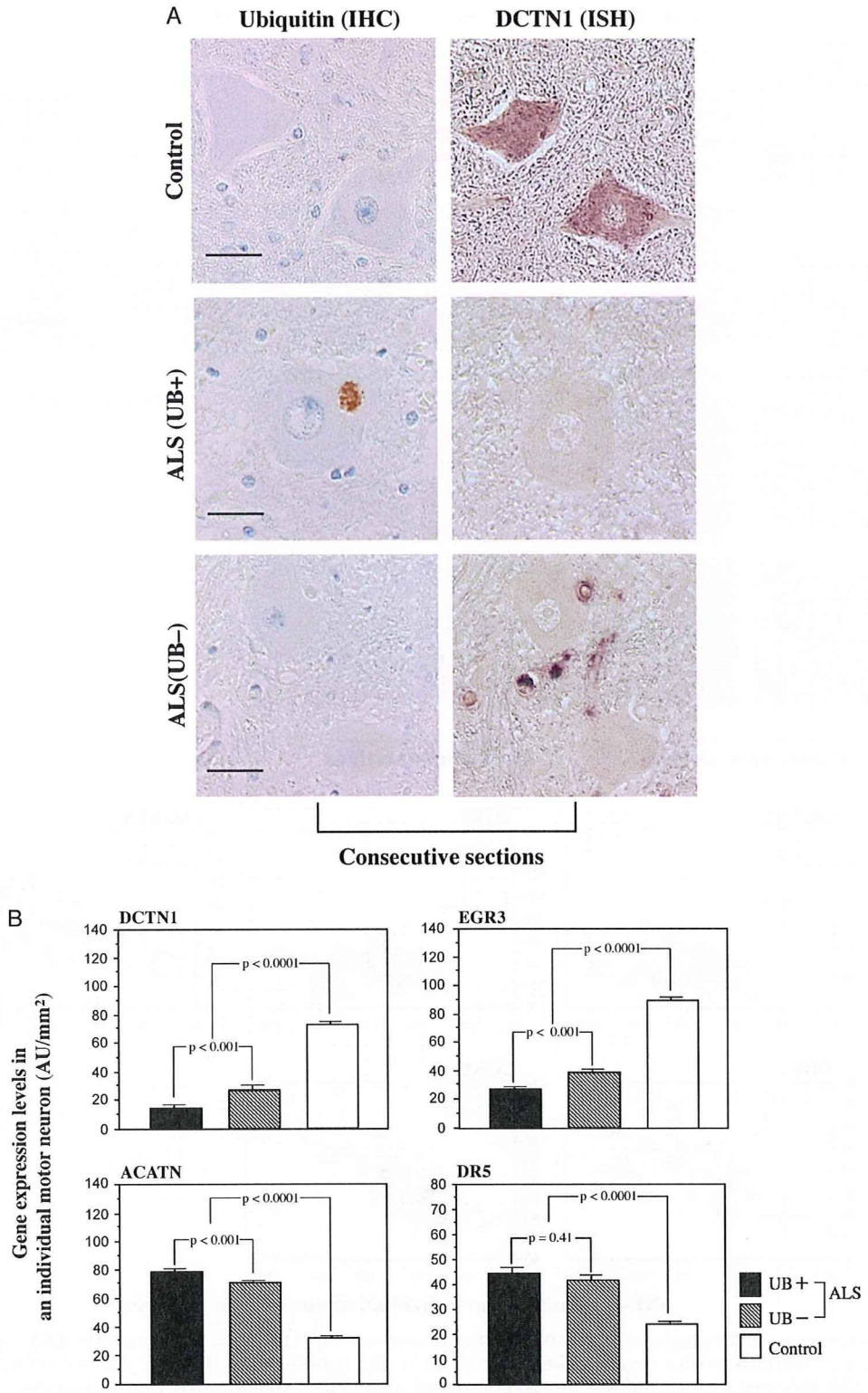


**FIGURE 4.** Gene expression and cytoplasmic accumulation of ubiquitylated proteins. **(A)** Representative *DCTN1* in situ hybridization (ISH) and ubiquitin (UB) immunohistochemistry (IHC) in identical motor neurons of consecutive sections are shown in patients with amyotrophic lateral sclerosis (ALS) and control patients. Scale bars = 25 μm. **(B)** Expression levels of genes were compared among the motor neurons that were either positive (n = 56) or negative (n = 175) for ubiquitylated proteins in 8 representative patients with ALS and those (n = 209) in 8 control patients. Expression levels of *DCTN1*, *EGR3*, and *ACATN* were significantly different in ubiquitin-positive compared to ubiquitin-negative neurons in ALS, whereas that of *DR5* was not. The values are shown as means ± SE. AU, arbitrary absorbance units.

a differential gene expression profile in isolated, laser-captured motor neurons from patients with sporadic ALS (15). Thus, we consider these gene expression levels to reflect most significantly the molecular events of neurodegeneration processes in motor neurons.

We selected 3 pathologic features as markers for neurodegeneration: the residual population of spinal motor neurons, cytoplasmic accumulation of pNF-H, and cytoplasmic accumulation of ubiquitylated proteins. Cytoplasmic accumulation of pNF-H has been demonstrated to occur in ALS motor neurons, even when they have normal morphologic appearances, and is thought to be a consequence of impaired axonal transport (5, 23–25). Hence, it is considered to be a histologic marker indicating neuronal degeneration and dysfunction before neuronal death (5, 16, 17). Hence, the accumulation of pNF-H is a rather early event in the motor neuron degeneration process. The presence of ubiquitylated proteins in the motor neuron cytoplasm has also been identified as a histopathologic marker of motor neuron degeneration (18). Ubiquitylated inclusions are thought to be aggregated, modified, and misfolded proteins that are ubiquitylated by motor neuron ubiquitin ligase (9). Although ubiquitylated, round inclusions are considered to occur in rather advanced stages of degeneration, it is not known whether dot-like and skein-like small faint ubiquitylated accumulations occur in the early stages of neurodegeneration.

The striking observation was that *DCTN1* expression was the most widely and most strongly downregulated among the genes examined in the residual motor neuron population, and was also severely downregulated even in the patients with large populations of motor neurons and in the motor neurons without pNF-H accumulations. The dramatic change in *DCTN1* in ALS seems to be specific for motor neurons because *DCTN1* expression was preserved in neurons in the dorsal nucleus of Clarke and the intermediolateral nucleus in the spinal cord, Purkinje cells of the cerebellum, and cortical neurons in the occipital cortex in patients with ALS. These observations suggest that *DCTN1* downregulation is the specific molecular event that occurs before the appearance of these pathologic markers, and is, therefore, a rather early event in the molecular sequences of neurodegeneration, at least among the events related to the genes examined. *DCTN1* codes for a protein that is a component of the retrograde transport protein complex with dynein (26, 27) and has been identified as a causative gene for human lower motor neuron disease (28, 29). Furthermore, it has been suggested that polymorphic amino acid substitution is a modifying factor accelerating pathogenesis and progression of sporadic ALS (30). A mouse model overexpressing dynamitin, which eventually results in late-onset progressive motor neuron degenerative disease, demonstrates the involvement of the dynactin-dynein complex (23). Two dominant point mutations in dynein cause progressive motor neuron degeneration in mice (31). These findings suggest that retrograde axonal transport involving the dynactin-dynein complex is strongly associated with motor neuron dysfunction and eventual motor neuron degeneration (32). By taking into account these findings, our present results strongly suggest that the downregulation of *DCTN1* in motor neurons may play a significant role in this process and may lead to the subsequent sequences of motor neuron degeneration in sporadic ALS. This hypothesis should be tested by further study on another cohort of patients with ALS and by in vitro and in vivo experiments.

Another interesting observation was that *ACATN*, *DR5*, and the CCNC protein were upregulated in subpopulations of residual motor neurons and that their upregulation was well correlated to the accumulation of pNF-H and the degree of motor neuron loss. ACATN functions as a cofactor for acetylation of gangliosides and has been demonstrated to suppress proapoptotic activity of GD3 ganglioside (33–36). In the *Drosophila* model, knockout of *ACATN* leads to a lethal phenotype owing to brain damage (Y. Hirabayashi, personal communication, 2007). DR5 is another cell death-related receptor as a member of the tumor necrosis factor (TNF) receptor family (TNFR10b) (37). CCNC is a cell cycle regulator protein and increases in *CCNC* expression are associated with its nuclear translocation, as was also demonstrated in this study (38). The aberrant activation of cell cycle regulators has been proposed as a pathway inducing motor neuron death in ALS (39, 40). Moreover, upregulated *DR5* was colocalized in motor neurons with CCNC nuclear translocation and also in those with downregulated TNFR-associated factor 6 (TRAF6) in our study (data not shown). The downregulated TRAF6, which is associated with nuclear factor-κB activation for cell survival, may not be able to sequester the overexpressed DR5 signaling, leading to a pathway of cell death (41). Taken together, expressions of these genes are involved in the cell death-related pathway. Upregulation of these genes occurs in subpopulations of motor neurons in parallel to or after the emergence of histopathologic markers such as pHF-H accumulation and motor neuron loss, suggesting that they occur in a relatively late phase of neurodegeneration, especially compared with *DCTN1* downregulation. The observation that active motor neuron degeneration processes for cell death that are probably mediated via cell death-related gene expression, such as *ACATN*, *DR5* and CCNC upregulation, occur in subpopulations of the remaining motor neurons with sustained *DCTN1* downregulation is consistent with our previous results that motor neurons in the remaining motor neuron pool randomly enter into the active degeneration process even up to the terminal stage in sporadic ALS (42).

The appearance of ubiquitylated protein accumulations or ubiquitylated inclusions is one of the hallmarks of motor neuron degeneration in sporadic ALS (18). In this study, however, the expression levels of *DCTN1*, *EGR3*, *ACATN*, and *DR5* were significantly altered before the appearance of ubiquitylated protein accumulations. Because the morphologic features of cytoplasmic ubiquitylated protein accumulations vary considerably, ranging from fine dot-like or skein-like accumulations to large inclusions, the simple assessment of ubiquitin-positive or negative materials may not be sufficient to identify neurodegeneration. However, even when we assessed ubiquitylated accumulation in a more precise manner, the expressions of these 4 genes were markedly altered independent of the appearance

of ubiquitylated protein accumulations. These findings suggest that appearance of ubiquitylated protein accumulation is a later pathologic event, occurring after the expressions of a number of genes are already altered. Alternatively, we may speculate that ubiquitylated protein accumulation is a secondary consequence of the series of molecular events accompanied by the alterations of a wide-range of gene expressions.

The present study also demonstrates that microarray analyses on laser-captured motor neurons followed by histopathologic analyses on tissues from large numbers of patients can provide significant information about molecular events in motor neuron degeneration and dysfunction in patients with sporadic ALS. The most serious problem in developing effective therapy for sporadic ALS is the lack of animal or cell models that properly reflect the motor neuron degeneration processes of sporadic ALS or even certain aspects of them. This is not a longitudinal and chronologic analysis of degeneration process in identical motor neurons, and it is not clear whether the changes seen in the present study represent the primary causes or secondary effects in the disease process because of the inherent problem of studying human disease using autopsy materials. However, we may be able to speculate that these results of human studies reflect the molecular sequence of motor neuron degeneration of ALS. Our present approach would provide an avenue for developing new molecular-targeted therapies for sporadic ALS by creating animal or cell models mimicking the molecular events seen in human patients.

## REFERENCES


1. Ince PG, Lowe J, Shaw PJ. Amyotrophic lateral sclerosis: Current issues in classification, pathogenesis and molecular pathology. Neuropathol Appl Neurobiol 1998;24:104–107
2. Bunina TL. On intracellular inclusions in familial amyotrophic lateral sclerosis. Korsakov J Neuropath Psychiatry 1962;62:1293–96
3. Okamoto K, Hirai S, Amari M, et al. Bunina bodies in amyotrophic lateral sclerosis immunostained with rabbit anti-cystatin C serum. Neurosci Lett 1993;162:125–28
4. Bergeron C. Oxidative stress: Its role in the pathogenesis of amyotrophic lateral sclerosis. J Neurol Sci 1995;129(Suppl):81–84
5. Cleveland DW, Rothstein JD. From Charcot to Lou Gehrig: Deciphering selective motor neuron death in ALS. Nat Rev Neurosci 2001;2:806–19
6. Sathasivam S, Ince PG, Shaw PJ. Apoptosis in amyotrophic lateral sclerosis: A review of the evidence. Neuropathol Appl Neurobiol 2001;27:257–74
7. Hand CK, Rouleau GA. Familial amyotrophic lateral sclerosis. Muscle Nerve 2002;25:135–59
8. Ishigaki S, Liang Y, Yamamoto M, et al. X-Linked inhibitor of apoptosis protein is involved in mutant SOD1-mediated neuronal degeneration. J Neurochem 2002;82:576–84
9. Niwa J, Ishigaki S, Hishikawa N, et al. Dorfin ubiquitylates mutant SOD1 and prevents mutant SOD1-mediated neurotoxicity. J Biol Chem 2002;277:36793–98
10. Hishikawa N, Niwa J, Doyu M, et al. Dorfin localizes to the ubiquitylated inclusions in Parkinson's disease, dementia with Lewy bodies, multiple system atrophy, and amyotrophic lateral sclerosis. Am J Pathol 2003;163:609–19
11. Kawahara Y, Ito K, Sun H, et al. Glutamate receptors: RNA editing and death of motor neurons. Nature 2004;427:801
12. Kunst CB. Complex genetics of amyotrophic lateral sclerosis. Am J Hum Genet 2004;75:933–47
13. Bruijn LI, Miller TM, Cleveland DW. Unraveling the mechanisms involved in motor neuron degeneration in ALS. Annu Rev Neurosci 2004;27:723–49
14. Ralph GS, Radcliffe PA, Day DM, et al. Silencing mutant SOD1 using RNAi protects against neurodegeneration and extends survival in an ALS model. Nat Med 2005;11:429–33
15. Jiang YM, Yamamoto M, Kobayashi Y, et al. Gene expression profile of spinal motor neurons in sporadic amyotrophic lateral sclerosis. Ann Neurol 2005;57:236–51
16. Manetto V, Sternberger NH, Perry G, et al. Phosphorylation of neurofilaments is altered in amyotrophic lateral sclerosis. J Neuropathol Exp Neurol 1988;47:642–53
17. Sobue G, Hashizume Y, Yasuda T, et al. Phosphorylated high molecular weight neurofilament protein in lower motor neurons in amyotrophic lateral sclerosis and other neurodegenerative diseases involving ventral horn cells. Acta Neuropathol (Berl) 1990;79:402–408
18. Strong MJ, Kesavapany S, Pant HC. The pathobiology of amyotrophic lateral sclerosis: A proteinopathy? J Neuropathol Exp Neurol 2005;64:649–64
19. Mitsuma N, Yamamoto M, Iijima M, et al. Wide range of lineages of cells expressing nerve growth factor mRNA in the nerve lesions of patients with vasculitic neuropathy: An implication of endoneurial macrophage for nerve regeneration. Neuroscience 2004;129:109–17
20. Yamamoto M, Li M, Mitsuma N, et al. Preserved phosphorylation of RET receptor protein in spinal motor neurons of patients with amyotrophic lateral sclerosis: An immunohistochemical study by a phosphorylation-specific antibody at tyrosine 1062. Brain Res 2001;912:89–94
21. Terao S, Sobue G, Hashizume Y, et al. Disease-specific patterns of neuronal loss in the spinal ventral horn in amyotrophic lateral sclerosis, multiple system atrophy and X-linked recessive bulbospinal neuronopathy, with special reference to the loss of small neurons in the intermediate zone. J Neurol 1994;241:196–203
22. Mizuno Y, Amari M, Takatama M, et al. Immunoreactivities of p62, an ubiquitin-binding protein, in the spinal anterior horn cells of patients with amyotrophic lateral sclerosis. J Neurol Sci 2006;249:13–18
23. LaMonte BH, Wallace KE, Holloway BA, et al. Disruption of dynein/dynactin inhibits axonal transport in motor neurons causing late-onset progressive degeneration. Neuron 2002;34:715–27
24. Kieran D, Hafezparast M, Bohnert S, et al. A mutation in dynein rescues axonal transport defects and extends the life span of ALS mice. J Cell Biol 2005;169:561–67
25. Lobsiger CS, Garcia ML, Ward CM, et al. Altered axonal architecture by removal of the heavily phosphorylated neurofilament tail domains strongly slows superoxide dismutase 1 mutant-mediated ALS. Proc Natl Acad Sci USA 2005;102:10351–56
26. King SJ, Schroer TA. Dynactin increases the processivity of the cytoplasmic dynein motor. Nat Cell Biol 2000;2:20–24
27. Schroer TA. Dynactin. Annu Rev Cell Dev Biol 2004;20:759–79
28. Puls I, Jonnakuty C, LaMonte BH, et al. Mutant dynactin in motor neuron disease. Nat Genet 2003;33:455–56
29. Puls I, Oh SJ, Sumner CJ, et al. Distal spinal and bulbar muscular atrophy caused by dynactin mutation. Ann Neurol 2005;57:687–94
30. Munch C, Sedlmeier R, Meyer T, et al. Point mutations of the p150 subunit of dynactin (*DCTN1*) gene in ALS. Neurology 2004;63:724–26
31. Hafezparast M, Klocke R, Ruhrberg C, et al. Mutations in dynein link motor neuron degeneration to defects in retrograde transport. Science 2003;300:808–12
32. Levy JR, Sumner CJ, Caviston JP, et al. A motor neuron disease-associated mutation in p150Glued perturbs dynactin function and induces protein aggregation. J Cell Biol 2006;172:733–45
33. Rapport MM, Donnenfeld H, Brunner W, et al. Ganglioside patterns in amyotrophic lateral sclerosis brain regions. Ann Neurol 1985;18:60–67
34. Kanamori A, Nakayama J, Fukuda MN, et al. Expression cloning and characterization of a cDNA encoding a novel membrane protein required for the formation of O-acetylated ganglioside: A putative acetyl-CoA transporter. Proc Natl Acad Sci USA 1997;94:2897–902
35. Bora RS, Ichikawa S, Kanamori A, et al. cDNA cloning of putative rat acetyl-CoA transporter and its expression pattern in brain. Cytogenet Cell Genet 2000;89:204–208
36. Malisan F, Franchi L, Tomassini B, et al. Acetylation suppresses the proapoptotic activity of GD3 ganglioside. J Exp Med 2002;196:1535–41

37. Milani D, Zauli G, Rimondi E, et al. Tumor necrosis factor-related apoptosis-inducing ligand sequentially activates pro-survival and pro-apoptotic pathways in SK-N-MC neuronal cells. J Neurochem 2003;86: 126–35
38. Ueberham U, Hessel A, Arendt T. Cyclin C expression is involved in the pathogenesis of Alzheimer's disease. Neurobiol Aging 2003;24:427–35
39. Nguyen MD, Boudreau M, Kriz J, et al. Cell cycle regulators in the neuronal death pathway of amyotrophic lateral sclerosis caused by mutant superoxide dismutase 1. J Neurosci 2003;23:2131–40
40. Ranganathan S, Bowser R. Alterations in $G_1$ to S phase cell-cycle regulators during amyotrophic lateral sclerosis. Am J Pathol 2003;162: 823–35
41. Foehr ED, Lin X, O'Mahony A, et al. NF-κB signaling promotes both cell survival and neurite process formation in nerve growth factor-stimulated PC12 cells. J Neurosci 2000;20:7556–63
42. Sobue G, Sahashi K, Takahashi A, et al. Degenerating compartment and functioning compartment of motor neurons in ALS: Possible process of motor neuron loss. Neurology 1983;33:654–57

Neurobiology of Disease

# CHIP Overexpression Reduces Mutant Androgen Receptor Protein and Ameliorates Phenotypes of the Spinal and Bulbar Muscular Atrophy Transgenic Mouse Model

**Hiroaki Adachi,[1] Masahiro Waza,[1] Keisuke Tokui,[1] Masahisa Katsuno,[1,2] Makoto Minamiyama,[1] Fumiaki Tanaka,[1] Manabu Doyu,[1] and Gen Sobue[1]**

[1]Department of Neurology, Nagoya University Graduate School of Medicine, Showa-ku, Nagoya 466-8550, Japan, and [2]Institute for Advanced Research, Nagoya University, Showa-ku, Nagoya 466-8550, Japan

Spinal and bulbar muscular atrophy (SBMA) is an inherited motor neuron disease caused by the expansion of a polyglutamine tract within the androgen receptor (AR). The pathologic features of SBMA are motor neuron loss in the spinal cord and brainstem and diffuse nuclear accumulation and nuclear inclusions of the mutant AR in the residual motor neurons and certain visceral organs. Many components of the ubiquitin-proteasome and molecular chaperones are also sequestered in the inclusions, suggesting that they may be actively engaged in an attempt to degrade or refold the mutant AR. C terminus of Hsc70 (heat shock cognate protein 70)-interacting protein (CHIP), a U-box type E3 ubiquitin ligase, has been shown to interact with heat shock protein 90 (Hsp90) or Hsp70 and ubiquitylates unfolded proteins trapped by molecular chaperones and degrades them. Here, we demonstrate that transient overexpression of CHIP in a neuronal cell model reduces the monomeric mutant AR more effectively than it does the wild type, suggesting that the mutant AR is more sensitive to CHIP than is the wild type. High expression of CHIP in an SBMA transgenic mouse model also ameliorated motor symptoms and inhibited neuronal nuclear accumulation of the mutant AR. When CHIP was overexpressed in transgenic SBMA mice, mutant AR was also preferentially degraded over wild-type AR. These findings suggest that CHIP overexpression ameliorates SBMA phenotypes in mice by reducing nuclear-localized mutant AR via enhanced mutant AR degradation. Thus, CHIP overexpression would provide a potential therapeutic avenue for SBMA.

*Key words:* CHIP; polyglutamine; SBMA; transgenic mice; protein degradation; androgen receptor

## Introduction

Polyglutamine (polyQ) diseases are inherited neurodegenerative disorders caused by the expansion of trinucleotide CAG repeats in the causative genes (Gatchel and Zoghbi, 2005). To date, nine polyQ diseases have been identified (Di Prospero and Fischbeck, 2005). One of these is spinal and bulbar muscular atrophy (SBMA), characterized by premature muscular exhaustion, progressive muscular weakness, atrophy, and fasciculation in bulbar and limb muscles (Kennedy et al., 1968; Sobue et al., 1993; Sperfeld et al., 2002; Atsuta et al., 2006). In SBMA, a polymorphic CAG repeat with 14–32 CAGs expands to 40–62 CAGs in the first exon of the androgen receptor (*AR*) gene (La Spada et al., 1991; Tanaka et al., 1996). CAG repeat size is inversely correlated with the age at onset and positively correlated with disease severity in SBMA (Doyu et al., 1992; Igarashi et al., 1992; La Spada et al., 1992). The histopathologic hallmarks of SBMA are lower motor neuronal loss (Sobue et al., 1989), diffuse nuclear accumulation, and nuclear inclusions (NIs) of expanded polyQ mutant AR in the residual motor neurons in brainstem and spinal cord as well as in some other visceral organs (Li et al., 1998a,b; Adachi et al., 2005). Such NIs are common pathological features in polyQ diseases and also colocalize with many components of the ubiquitin-proteasome and molecular chaperones (Adachi et al., 2001; Schmidt et al., 2002; Ross and Poirier, 2004), raising the possibility that the ubiquitin-proteasome system and molecular chaperones may actively attempt to degrade or refold components of the inclusions (Stenoien et al., 1999; Ross and Pickart, 2004). Furthermore, these proteasomes and chaperones should also facilitate refolding or proteolysis of toxic misfolded proteins (McClellan et al., 2005) and may play a role in protecting neuronal cells against the toxic properties of expanded polyQ (Cummings et al., 1998; Kobayashi et al., 2000).

C terminus of heat shock cognate protein 70 (Hsc70)-interacting protein (CHIP) has three tetratricopeptide repeat (TPR) domains that interact with the molecular chaperones heat shock protein 70 (Hsp70) and Hsp90 (Ballinger et al., 1999; Connell et al., 2001) and a U-box domain that interacts with the proteasome, conferring CHIP with E3 ubiquitin ligase activity

Received Dec. 25, 2006; accepted April 4, 2007.

This work was supported by a Center of Excellence grant and KAKENHI (17025020) from the Ministry of Education, Culture, Sports, Science, and Technology, Japan; by Special Coordination Funds for Promoting Science and Technology from the Ministry of Education, Culture, Sports, Science, and Technology, Japan; and by grants from the Ministry of Health, Labor, and Welfare, Japan. We have no financial conflict of interest that might be construed to influence the results or interpretation of this manuscript. We thank Jun-ichi Miyazaki for kindly providing the pCAGGS vector and Keiji Tanaka for the pcDNA3-CHIP vector.

Correspondence should be addressed to Dr. Gen Sobue, Department of Neurology, Nagoya University Graduate School of Medicine, 65 Tsurumai-cho Showa-ku, Nagoya 466-8550, Japan. E-mail: sobueg@med.nagoya-u.ac.jp.

DOI:10.1523/JNEUROSCI.1242-07.2007

 0270-6474/07/275115-12$15.00/0

(Hatakeyama et al., 2001; Jiang et al., 2001). Wild-type AR is one of the CHIP substrates (Cardozo et al., 2003; He et al., 2004). CHIP also interacts with misfolded proteins trapped by molecular chaperones and degrades them, thus acting as a "quality control" E3 (Cyr et al., 2002; Murata et al., 2003). In fact, CHIP suppressed inclusion formation and cellular toxicity in cell, zebrafish, and *Drosophila* polyQ disease models (Jana et al., 2005; Miller et al., 2005; Al-Ramahi et al., 2006).

In this study, we examine whether CHIP exerts therapeutic effects on a cultured cell model and a transgenic mouse model expressing the mutant AR to explore a potential strategy for SBMA therapy. We report that CHIP markedly ameliorated motor and pathological phenotypes and that this amelioration was correlated with the reduction of monomeric mutant AR and mutant AR protein complexes in the SBMA models.

## Materials and Methods

*Cell culture.* SH-SY5Y cells were transfected using Lipofectamine 2000 (Invitrogen, Carlsbad, CA) with plasmids encoding ARs containing normal (24 CAGs) or expanded (65 CAGs) polyQ repeats (Waza et al., 2005). Stable clones expressing these normal and mutant ARs were established by selection with the antibiotic G418 (0.4 mg/ml final concentration). The androgen receptor is not expressed in untransfected SH-SY5Y cells. All cell cultures were propagated in the absence of androgen. In Western blots from these cultures, we detected a band of monomeric mutant AR in the separating gel but could hardly detect the high-molecular-weight mutant AR protein complex, which was retained in the stacking gel. Therefore, this cultured cell model is better suited for estimating the change in monomeric mutant AR expression. There was no difference in viability between cells expressing the wild-type and mutant ARs in the absence of androgen using the CellTiter 96 AQueous One Solution Cell Proliferation Assay (Promega, Madison, WI).

*DNA transfection.* Plasmid pcDNA3-CHIP, encoding FLAG-tagged human CHIP, was kindly provided by Dr. Keiji Tanaka (Laboratory of Frontier Science, Tokyo Metropolitan Institute of Medical Science, Tokyo, Japan) (Murata et al., 2001). AR stable cells were plated in six-well dishes in 2 ml of DMEM/F-12 containing 10% charcoal-stripped fetal bovine serum with penicillin and streptomycin, and each dish was transfected with 4 μg of the vector containing CHIP or mock (negative control) using Lipofectamine 2000 according to the manufacturer's instructions. Transfection efficiency was 60–70%. The cells were cultured for 48 h at 37°C under 5% $CO_2$.

*Transgene construction.* Full-length human CHIP cDNA was generated from total RNA extracted from SH-SY5Y cells by reverse transcription-PCR. Full-length human CHIP was constructed by subcloning CHIP inserts derived from the full-length human CHIP cDNA into the pcDNA3.1-myc-his mammalian expression vector (Invitrogen) using PCR. Then, the myc-tagged CHIP fragments were subcloned into the pCAGGS vector (Niwa et al., 1991). All constructs were confirmed by DNA sequence analysis. The final plasmids were digested to remove the transgene.

*Generation and maintenance of Tg mice and genotyping.* We generated CHIP overexpression mice by microinjection of the transgene into BDF1 fertilized eggs and obtained four founders. BDF1 homozygous CHIP transgenic females were mated with BDF1/B6 male mice expressing full-length human AR with 24 (AR-24Q mice, 5-5 line) or 97-polyQ tracts (AR-97Q mice, 7-8 line), producing a mixed BDF1 and B6 genetic background. First-generation AR-24Q/CHIP$^{(tg/-)}$ or AR-97Q/CHIP$^{(tg/-)}$ mice were mated with either CHIP$^{(tg/-)}$ or CHIP$^{(tg/tg)}$ mice to produce all AR or AR/CHIP double-transgenic mice for each analysis. We screened mouse tail DNA by PCR for the presence of the transgene using the primers 5′-CATCTCAGAAGAGGATCTGTG-3′ and 5′-GGTCGAGGGATCTTCATAAG-3′.

*Neurological and behavioral assessment of SBMA model mice.* The AR-24Q and AR-97Q mice were generated and maintained as described previously (Katsuno et al., 2002). All animal experiments were performed in accordance with the National Institutes of Health *Guide for the Care and Use of Laboratory Animals* and under the approval of the Nagoya University Animal Experiment Committee. The AR-97Q male mice showed progressive muscular atrophy and weakness as well as diffuse nuclear staining and NIs of the mutant AR. These phenotypes were very pronounced in male transgenic mice, similar to the situation in SBMA patients. The mouse rotarod task (Economex Rotarod; Ugo Basile, Comerio, Italy) was performed on a weekly basis, and cage activity was measured weekly with the AB system (Neuroscience, Tokyo, Japan) as described previously (Katsuno et al., 2002; Minamiyama et al., 2004). Spontaneous motor activity was monitored for 24 h periods; all spontaneous movements, both vertical and horizontal, including locomotion, rearing, and head movements, were counted and automatically totaled.

*Immunohistochemistry and histopathology.* Mice were deeply anesthetized with ketamine–xylazine and transcardially perfused with 20 ml of 4% paraformaldehyde fixative in phosphate buffer, pH 7.4. Spinal cord and skeletal muscle tissues were removed, postfixed overnight in 10% phosphate-buffered formalin, and processed for paraffin embedding. Sections (6 μm thick) of the above tissues were deparaffinized, dehydrated with alcohol, and treated in formic acid for 5 min at room temperature. For the immunohistochemical studies, the paraffin sections were preheated in a microwave oven for 10 min. The sections were blocked with normal animal serum (1:20) and incubated with mouse anti-expanded polyQ antibody (1:10,000; 1C2; Millipore, Billerica, MA), anti-CHIP antibody (1:1000; Medical and Biological Laboratories, Nagoya, Japan), and mouse anti-glial fibrillary acidic protein (GFAP) antibody (1:1000; Roche Diagnostics, Mannheim, Germany). Primary antibodies were probed with a biotinylated anti-species-specific IgG (Vector Laboratories, Burlingame, CA), and the immune complexes were visualized using streptavidin-horseradish peroxidase (Dako, Glostrup, Denmark) and 3,3′-diaminobenzidine (Dojindo, Kumamoto, Japan) as a substrate. Sections were counterstained with Mayer's hematoxylin. Paraffin-embedded sections (6 μm thick) of the gastrocnemius muscles were air dried and stained with hematoxylin and eosin. For double-immunofluorescence staining of the spinal cord, sections were blocked with 5% normal goat serum and then sequentially incubated with anti-CHIP antibody (1:1000; Medical and Biological Laboratories) and 1C2 antibody (1:10,000; Millipore) at 4°C overnight. The sections were then incubated with Alexa 488-conjugated goat anti-chicken IgG (1:1000; Invitrogen) and Alexa 568-conjugated goat anti-mouse IgG (1:1300; Invitrogen) for 8 h at 4°C. The stained sections were examined and photographed with a confocal laser-scanning microscope (LSM 5 PASCAL; Carl Zeiss MicroImaging, Tokyo, Japan).

*Patients.* Tissue from nine patients with clinicopathologically and genetically confirmed SBMA (51–84 years of age; mean, 64.3 years), and three non-neurological controls (51–76 years of age; mean, 64.0 years) were also used in the present study. These patients had been hospitalized and followed up at Nagoya University Hospital and its affiliated hospitals during the past 25 years. Informed consent was obtained to use the tissues for research purposes. Paraffin-embedded sections of the spinal cord and brain were obtained and examined in the same way as those from transgenic mice.

*Quantification of 1C2-positive cells.* For assessment of 1C2-positive cells in the ventral horn of the spinal cord, 50 consecutive transverse sections of the thoracic spinal cord were prepared from each individual mouse, and 1C2-positive cells within the ventral horn of every fifth section were counted as described previously (Adachi et al., 2001). Populations of 1C2-positive cells were expressed as number/mm$^2$. For assessment of 1C2-positive cells in muscle, the number of 1C2-positive cells was calculated from counts of >500 fibers in randomly selected areas of individual mice and expressed as the number per 100 muscle fibers. The quantitative data of six individual mice were expressed as mean ± SEM.

*Protein expression analysis and ubiquitination assay.* Forty-eight hours after transfection, cells were lysed in CelLytic-M Mammalian Cell Lysis/Extraction Reagent (Sigma, St. Louis, MO) with 1 mM PMSF and 6 μg/ml aprotinin and centrifuged at 15,000 × *g* for 15 min at 4°C. Sixteen-week-old mice were exsanguinated under ketamine–xylazine anesthesia, and tissues were snap frozen with powdered $CO_2$ in acetone. The tissues were homogenized in CelLytic-M Mammalian Cell Lysis/Extraction Reagent (Sigma) with 1 mM PMSF and 6 μg/ml aprotinin and centrifuged at